

# A Unified Error Correction Code for Universal Quantum Computing with Identical Particles

S. L. Wu<sup>1,2</sup> and Lian-Ao Wu<sup>2,3,4,\*</sup>

<sup>1</sup>*School of Physics and Materials Engineering, Dalian Nationalities University, Dalian 116600 China*

<sup>2</sup>*Department of Physics, University of the Basque Country UPV/EHU, 48080 Bilbao, Spain*

<sup>3</sup>*IKERBASQUE Basque Foundation for Science, 48013 Bilbao, Spain*

<sup>4</sup>*EHU Quantum Center, University of the Basque Country UPV/EHU, Leioa, Biscay 48940, Spain*

(Dated: February 25, 2026)

We present a universal fault-tolerant quantum computing architecture based on identical particle qubits (IPQs), where we find that the first-order IPQ - bath interaction fundamentally differs from the conventional first-order qubit-bath interaction. This key distinction necessitates a redesign of existing strategies to fight decoherence. We propose that the simplest quantum error correction code can be realized directly within the physical qubit, provided that conventional correction and restoration are generalized beyond unitary operations to employ physically implementable reversal operations - naturally placing logical and physical qubits on equal footing. We further demonstrate that dynamical decoupling (DD) remains effective within this unified framework, and that a decoherence-free subspace (DFS)-like structure emerges. Unlike previous approximate treatments, our analytically solvable IPQ-Bath model enables rigorous testing of these strategies, with numerical simulations validating their effectiveness.

## I. INTRODUCTION

Quantum decoherence remains the primary obstacle to realizing practical quantum computers, making error correction and suppression essential challenges in their development [1]. Several strategies to fight decoherence, including the closed-loop QEC, open-loop DD and DFS, have been proposed and implemented based on first-order qubit-bath interactions across various physical platforms [2–6]. Closed-loop QEC theories and practices aim to protect quantum information by encoding logical qubits into larger Hilbert spaces including multi-qubit space and Bosonic space, such as the surface code, color codes, concatenated codes, and bosonic binomial codes to enable continuous-variable systems for hardware-efficient protection against photon loss [7]. In recent years, experimental progress has accelerated significantly: repeated error correction using stabilizer codes has demonstrated logical error rates well below physical rates on trapped-ion platforms [10], while bosonic codes, including cat and binomial codes, have been successfully implemented in superconducting cavities with concatenated architectures [11], and error correction with high-dimensional bosonic binomial code [12] and GKP codes [13]. These efforts highlight both the diversity of QEC strategies and the growing maturity of fault-tolerant operations across platforms, although extending the lifetimes of encoded logical qubits beyond those of the best available physical qubits remains elusive, as noted in [12].

In this work, we investigate a general scheme that encodes qubits using identical particles, where quantum information is stored in two quantum states or levels, each occupied by one of two identical particles. This iden-

tical particle qubit scheme leverages intrinsic degrees of freedom, similar to encoding in cold atoms [3, 16–18] or dual-rail representations in the linear optical quantum computing [14, 15, 17, 19, 20]. Such a scheme has demonstrated favourable performance against errors and improved robustness against Pauli errors and applications [21–24]. Unusually, we find that the first-order system-bath (IPQ-B) interaction in IPQ setting differs fundamentally from the conventional first-order qubit-bath interaction assumed in standard error correction schemes. As a result, conventional approaches to fight decoherence and noise, including QECCs, must be redesigned or reformulated to account for the structure of the first-order IPQ-B interaction.

Our analysis reveals that the simplest QECC is naturally realized by the IPQ itself, where system errors can be detected by measuring the parity of the IPQ [25–27]. However, as a code, the IPQ does not satisfy the standard QEC criteria when errors arise from the first-order IPQ-B interaction. Rather than relying on a unitary recovery operation, here we propose using a physically realizable reversal process implemented through a joint unitary operation on the IPQ and an ancillary qubit, followed by measurement of the ancilla. Furthermore, this first-order IPQ-B interaction leads to analytically solvable dynamics and reveals exact symmetries even when IPQs are embedded in an environment. We identify a DFS-like and associated gate operations that are inherently robust against such interactions [28].

Dynamical decoupling is effective for IPQs: leakage-elimination operators (LEOs) commute with—and are independent of—the universal gate set, so control adds no extra errors [30, 31]; DD performance is strong in practice [29]. Under suitable conditions this framework can eliminate quantum noise, enabling a unified code that integrates QECC, DD, and DFS for a robust, scalable route to fault-tolerant quantum computing with identi-

---

\* lianao.wu@ehu.es

cal particles.

In this Article, we introduce an identical-particle qubit (IPQ) encoding that stores one logical qubit in two modes occupied by a single identical particle. We first present the encoding and its controllable generators, then analyze its error-correction properties and compare it with representative bosonic encodings. We next study the system-bath dynamics in closed form, identify how collective and individual reservoirs affect both the encoded subspace and leakage, and show how leakage-elimination operators (LEOs) suppress the dominant error channels. Finally, we discuss a two-qubit gate implementation and quantify its performance in the presence of finite-temperature noise.

The paper is organized as follows. Section II introduces the encoding, its generators, and its error-correction features, together with comparisons and performance benchmarks. Section III presents the main dynamical results for the IPQ coupled to bosonic environments and the resulting control protocols. Section IV analyzes individual reservoirs and presents numerical results. Technical derivations are collected in the Appendices.

## II. IDENTICAL-PARTICLE QUBITS AS A SELF-PROTECTED ERROR-CORRECTING ENCODING

In this section we define the IPQ encoding and the associated controllable generators, and then characterize its error-correction properties in a form parallel to standard qubit QECCs. We also compare the IPQ with representative bosonic encodings to clarify when identical-particle hardware offers an advantage.

### A. Encoding and generators

We consider a system comprising two modes of identical particles with creation operators  $c_0^\dagger$  and  $c_1^\dagger$ . The information is encoded in the two states as a qubit, specifically an identical particle qubit (IPQ) spanned by  $|0\rangle = c_0^\dagger|\text{vacuum}\rangle$  and  $|1\rangle = c_1^\dagger|\text{vacuum}\rangle$ , where  $|\text{vacuum}\rangle$  denotes the vacuum state. This scheme has been exemplified by two-component bosons or fermions [3, 33], such as in the dual-rail encoding optical photon proposal [14, 17], and formulated in general [34]. It can be also a cold atom system trapped in optical lattices, where information can be encoded in the intrinsic degrees of freedom of the cold atoms.

Single-qubit gate operations are generated by [34],

$$J_x = c_0^\dagger c_1 + c_1^\dagger c_0, \quad J_z = c_0^\dagger c_0 - c_1^\dagger c_1, \quad (1)$$

and  $J_y = i[J_x, J_z]$ . Together these operators form an  $su(2)$  algebra [35], whose two-dimensional representations are Pauli matrices. Physical realizations include cold atom systems [3], circuit quantum electrodynamics systems [36] and superconducting cavities etc. [37–40].

With the encoding and controllable generators in place, we now summarize the error-correction properties of the IPQ and provide comparisons with standard bosonic encodings.

### B. Error-correction properties of the IPQ

Quantum error correction codes (QECCs) are designed based on the first-order qubit-bath interaction [41]. The total qubit-bath Hamiltonian is given by  $H = H_S + H_B + H_{SB}$ , where  $H_S$  and  $H_B$  represent the qubit and bath Hamiltonians. In general, the interaction  $H_{SB} = \vec{\sigma} \cdot \vec{B}$  is the lowest/first order of the qubit-bath interaction, which results in Pauli errors. The interaction is assumed to be dominant in the design of quantum error correction schemes [42–44]. The second order interactions are described by a second-rank tensor [32].

Analogous to the expansion in terms of Pauli operators, the lowest order expansion of  $H_{SB}$  for an IPQ is given by:

$$H_{SB} = \sum_{i=0,1} (c_i^\dagger B + c_i B^\dagger), \quad (2)$$

where the two bosons  $c_0^\dagger$  and  $c_1^\dagger$  must be embedded in a common environment; otherwise, the naturally occurring relaxation between them would not be captured by the first-order IPQ-B interaction. The Appendix demonstrates this relaxation numerically due to the first-order IPQ-B interaction.

The second order in Bosonic expansion may correspond to the conventional qubit-bath interaction  $\vec{J} \cdot \vec{B}'$  or in the conventional notation  $\vec{\sigma} \cdot \vec{B}$ , which essentially results from the dipole approximation and  $B'$  has the same form as  $B$ . In the present theoretical framework, the Pauli errors involve three bosonic or fermionic operators, for example,  $c_0^\dagger c_1 (b_\alpha^\dagger + b_\alpha)$ , which is a *nonlinear* term and has the same form and order as spontaneous parametric down-conversion in quantum optics. Therefore the first order expansion Eq. (2) is supposed to be significantly stronger than the second order expansion.

Analogous to the standard QEC theory, which is based on the first-order interaction  $\vec{\sigma} \cdot \vec{B}$ , the codewords for IPQs should be specifically designed to address the first-order IPQ-B interaction (2). Theoretically it is more similar to the simplest binomial code [7] than the conventional multi-qubit QECCs. A standard QECC facilitates the detection and correction of quantum errors by encoding quantum information into a protected subspace [45]. Its main purpose is to recover the quantum state to its original form after errors occur.

Consider the dipole-dipole interaction, the system-bath interaction is simplified as  $H_{SB} = (x_1 + x_0)B$  with  $x_i = (c_i^\dagger + c_i)/\sqrt{2}$ . In this case, we will demonstrate that the simplest QECC corresponds directly to the IPQ itself, provided that conventional correction and restora-

TABLE I. The QEC code with single qubit.

Measure Result	Error	Recovery Method
+1	none	$I$
-1	$x_1 + x_0$	MAQ WWM

tion are generalized beyond unitary operations to employ physically implementable reversal operations.

First, the error syndromes are detected by the parity or Stabilizer generator  $(-1)^{n_1+n_2+1}$ , where  $n_i = c_i^\dagger c_i$ , representing the parity measurement performed on the IPQs [25]. Unfortunately, unlike the simplest binomial encoding, the codewords  $|0\rangle$  and  $|1\rangle$  do not satisfy the QEC criteria (Knill-Laflamme conditions) [7] and correction cannot be made by unitary recovery. We now propose a different method for correction and restoration. It is straightforward that no correction to the IPQ system is required when the parity measurement indicates odd parity. Otherwise when the parity is even, the state with error will be  $\varepsilon x|\psi\rangle$  and cannot be corrected using the standard QEC method, where  $|\psi\rangle = a|0\rangle + b|1\rangle$  is an arbitrary IPQ state and  $x = x_1 + x_0$  is the error with dimensionless error strength  $\varepsilon$ . To address this, we now propose an innovative scheme, using a well developed technique [8, 9], for error correction by introducing an ancillary qubit initialized in the state  $|0_q\rangle$  such that the total state is given by their tensor product  $\varepsilon x|\psi\rangle|0_q\rangle$ . Next, we apply the following unitary transformation on the combined system  $U = \frac{1}{\varepsilon x}(|0_q\rangle\langle 0_q| + |1_q\rangle\langle 1_q|) + \sqrt{1 - \frac{1}{\varepsilon^2 x^2}}(|1_q\rangle\langle 0_q| - |0_q\rangle\langle 1_q|)$ , and then measure the ancillary qubit. If the measurement of the ancillary qubit (MAQ) yields  $|0_q\rangle$ , then  $\langle 0|U|0\rangle\varepsilon x|\psi\rangle = |\psi\rangle$ , indicating that the error is corrected. If the MAQ is  $|1_q\rangle$ , the IPA state becomes  $\langle 1|U|0\rangle\varepsilon x|\psi\rangle = i\sqrt{1 - \varepsilon^2 x^2}|\psi\rangle$ . For small  $\varepsilon$ , we have approximately  $\langle 1|U|0\rangle|\psi_c\rangle \approx i|\psi\rangle$ , which means the first-order error is also corrected. This makes the scheme a win-win measurement (WWM), as either measurement outcome can effectively correct the error. Essentially, the proposed QEC is equivalent to applying the inverse transform  $\frac{1}{x}$  on the error states, enabling immediate recovery since  $\frac{1}{x}x|\psi\rangle = |\psi\rangle$ , where the reserve recovery  $\frac{1}{x}$  is implemented by the joint unitary operation  $U$  plus ancillary measurement.

As for the break-even point, our scheme is similar to the bosonic binomial codes, where *beating the breaking-even point* is defined as achieving a logical qubit lifetime longer than the best available physical qubit lifetime and demonstrated experimentally in [12] and [13]. In our case, where the IPQ serves as both the physical and logical qubit, beating the break-even point means surpassing the intrinsic lifetime of the IPQ itself. In addition, errors introduced by the measurement of the ancillary qubit must also be taken into account.

## C. Comparison with binomial bosonic codes

To place the IPQ in context, we next benchmark it against commonly used bosonic encodings and discuss the conditions under which the IPQ reaches or surpasses a break-even point.

### 1. Binomial code

To illustrate the essential idea of the binomial quantum code and its connection to the Knill-Laflamme condition, we consider the simplest case that corrects a single photon-loss error. The Knill-Laflamme criterion for a code space  $\{|W_0\rangle, |W_1\rangle\}$  with an error set  $\{E_k\}$  requires

$$\langle W_i|E_i^\dagger E_k|W_j\rangle = C_{lk} \delta_{ij}, \quad (3)$$

with constants  $C_{lk}$  independent of the logical indices  $i, j$ . This ensures that different logical states remain orthogonal under errors, and that the logical information is preserved and can be recovered by unitary operations.

As a concrete example, we encode the logical qubit as

$$|W_0\rangle = \frac{|0\rangle + |4\rangle}{\sqrt{2}}, \quad |W_1\rangle = |2\rangle, \quad (4)$$

where  $|n\rangle$  are the Fock states, so that any logical state  $|\psi\rangle = u|W_0\rangle + v|W_1\rangle$  occupies only even photon-number states. A single photon-loss error  $a$  maps the logical words into orthogonal odd subspaces,

$$a|W_0\rangle = |3\rangle, \quad a|W_1\rangle = |1\rangle, \quad (5)$$

so that parity measurement

$$P = e^{i\pi\hat{n}}, \quad P|n\rangle = (-1)^n|n\rangle \quad (6)$$

directly reveals whether an error has occurred by distinguishing even and odd photon numbers.

If an error is detected, a unitary operation

$$U|3\rangle = |0\rangle, \quad U|1\rangle = |2\rangle \quad (7)$$

maps the state back to the original code space, restoring the initial logical qubit.

### 2. IPQ versus binomial code

In this subsection, we compare the IPQ code and the binomial code from different perspectives, including the error Hamiltonian, error detection methods, and error correction strategies.

First, both the IPQ code and the binomial code are bosonic codes built upon bosonic systems. The difference lies in the fact that the IPQ code requires two bosonic modes, whereas the binomial code only involves a single mode. As a result, the types of errors in the two codes

differ significantly. For the binomial code, the system–bath interaction takes the form

$$H_{SB}^B = aB^\dagger + a^\dagger B, \quad (8)$$

so single-photon loss and gain processes are the dominant sources of errors. These errors belong to the class of logical errors. In contrast, for the IPQ code, the system–bath interaction reads

$$H_{SB} = \sum_{i=0,1} (c_i^\dagger + c_i) B_1 + \sum_{i,j} (c_i^\dagger c_j B_2 + c_i c_j^\dagger B_2^\dagger). \quad (9)$$

The dominant contribution comes from the first term, corresponding to dipole-dipole interactions between single identical particles and the environment. Such errors do not alter the logical encoding but only modify the computational basis states. Therefore, they do not lead to any logical errors. Logical errors arise from the second term, which is nonlinear and involves three-operator interactions, so its strength is much weaker than that of the first term. Therefore, the IPQ code exhibits strong robustness against logical errors.

In terms of error detection, the two methods are similar. A non-destructive parity measurement is performed to monitor whether the system parity changes; a change in parity indicates that an error has occurred. For the IPQ code, a joint parity measurement over all IPQs is required. We do not need to identify which bosonic mode experienced the error, since the errors in the IPQ code originate from dipole-type interactions between the system and the environment rather than from single excitation loss or gain processes. Consequently, the IPQ code can be corrected even when the Knill–Laflamme condition is not strictly satisfied.

In terms of error correction, the binomial code satisfies the Knill–Laflamme condition and thus allows for the correction of logical errors via unitary transformations. On the other hand, a straightforward calculation shows that the IPQ code does **not** satisfy the Knill–Laflamme condition. To address this, we design a **non-unitary** correction scheme aimed at correcting computational basis errors. Since such errors are not logical errors, the non-unitary correction does not affect the logical encoding, which is precisely the motivation behind our scheme. Specifically, we introduce an auxiliary two-level system prepared in the state  $|0_a\rangle$ . Whenever the parity measurement signals the occurrence of an error, the erroneous code of the total system can always be written as

$$|E_0\rangle = \begin{pmatrix} \varepsilon x(a|0\rangle + b|1\rangle) \\ 0 \end{pmatrix}, \quad (10)$$

expressed in the orthonormal basis  $\{|0_a\rangle, |1_a\rangle\}$  of the auxiliary system. Then, the IPQ system and the auxiliary qubit undergo the following unitary operation

$$U = \begin{pmatrix} \frac{1}{\varepsilon x} & \sqrt{1 - \frac{1}{\varepsilon^2 x^2}} \\ \sqrt{1 - \frac{1}{\varepsilon^2 x^2}} & \frac{1}{\varepsilon x} \end{pmatrix}, \quad (11)$$

which leads to

$$|F_0\rangle = U|E_0\rangle = \begin{pmatrix} a|0\rangle + b|1\rangle \\ \sqrt{\varepsilon^2 x^2 - 1}(a|0\rangle + b|1\rangle) \end{pmatrix}. \quad (12)$$

For  $\varepsilon \ll 1$ , we have

$$|F_0\rangle \begin{pmatrix} a|0\rangle + b|1\rangle \\ i(a|0\rangle + b|1\rangle) \end{pmatrix}. \quad (13)$$

After performing the measurement on the auxiliary system, we readily find that the computational basis errors are corrected regardless of the measurement outcome.

In summary, although both the IPQ code and the binomial code are bosonic codes, they constitute two independent coding schemes. The binomial code satisfies the Knill–Laflamme condition and corrects logical errors arising from photon loss and gain through appropriately designed unitary transformations. In contrast, for the IPQ code, logical errors are associated with nonlinear interactions and thus occur only rarely; instead, the dominant errors are computational basis errors. This allows us to employ a non-unitary correction scheme to eliminate computational basis errors without disturbing the logical encoding.

#### D. Toward the break-even point with identical-particle qubits

The notion of a *break-even point* in quantum error correction refers to the condition where the lifetime of a protected logical qubit equals or surpasses that of the best physical qubit in the same platform,

$$\tau_L \geq \tau_P, \quad (14)$$

marking the onset where active error correction provides a net benefit rather than additional overhead. In bosonic codes such as cat and binomial encodings, this threshold has been reached only marginally—for instance, the experiment of Grimm *et al.* achieved  $\tau_L/\tau_P \simeq 1.16$ —because their dominant noise channels arise *within* the encoded subspace through spin-like couplings of the form

$$H_{SB}^{(\text{spin})} = \sum_i \sigma_i \cdot \mathbf{B}_i, \quad (15)$$

which act directly on logical degrees of freedom. Consequently, even perfect correction of photon-loss events cannot eliminate logical bit-flip and dephasing errors that originate intrinsically in the microscopic Hamiltonian.

In contrast, the identical-particle qubit (IPQ) framework introduced here fundamentally alters this microscopic structure. The first-order system–bath coupling takes a *collective bilinear* form, i.e., the first term in Eq.(2) which preserves the logical basis and shifts all leading logical errors to higher orders in the coupling strength. This microscopic suppression, combined with

the measurement-assisted nonunitary recovery and the leakage-elimination operator (LEO) protection, effectively removes the primary logical error channel rather than merely correcting its consequences.

Therefore, the IPQ scheme provides a *hardware-level route* toward surpassing the break-even point. Because logical coherence is preserved already at the interaction level, the logical lifetime  $\tau_L$  can, in principle, exceed the physical particle lifetime even *without* repeated parity-check cycles. The unified framework of QECC, DD, and DFS developed here allows the break-even threshold to be crossed *passively*, through intrinsic error prevention instead of frequent active correction. This conceptual shift—from “detect and correct” to “prevent and preserve”—represents a distinct pathway to scalable, fault-tolerant quantum computation with identical particles.

### E. IPQ code versus dual-rail code

The present interaction Hamiltonian differs fundamentally from that of the dual-rail encoding. In our framework, the system-bath coupling takes the collective-coordinate form

$$H_{SB} = xB, \quad (16)$$

where  $x = x_1 + x_2$  that jointly interact with a common reservoir. Because the constituent particles are identical, the coupling is symmetric under particle exchange and induces a collective decoherence process. Such collective interaction preserves the symmetry of the total wave function and confines the dynamics to a symmetric logical manifold. Errors generated by this  $xB$ -type coupling correspond to collective displacements or phase distortions, which mix logical states within the same subspace and can, in principle, be deterministically corrected through the nonunitary inverse operation discussed below.

In contrast, the dual-rail architecture is built on two physically distinct and addressable modes. Each mode couples independently to its own bath, leading to the energy-exchange interaction

$$H_{SB}^{(\text{DR})} = \sum_{i=0,1} (a_i B_i^\dagger + a_i^\dagger B_i), \quad (17)$$

where  $a_i$  annihilates a photon in the  $i$ th rail and  $B_i$  represents the corresponding environmental operator. The logical basis of the dual-rail qubit,  $|0_L\rangle = |1, 0\rangle$  and  $|1_L\rangle = |0, 1\rangle$ , is defined by a single photon occupying one of two separable modes. When photon loss occurs in either rail, the system is driven to the vacuum state  $|0, 0\rangle$ , leaving the logical subspace. Such independent, mode-specific interactions correspond to individual decoherence, allowing erasure detection but preventing full state recovery.

The relation between the two models can be established in specific limits. When the rotating-wave approximation (RWA) is applied to the  $xB$ -type coupling, the

fast-oscillating counter-rotating terms  $cB$  and  $c^\dagger B^\dagger$  are neglected, and the interaction effectively reduces to an energy-exchange form proportional to  $cB^\dagger + c^\dagger B$ . If, in addition, the system modes couple to distinct reservoirs rather than to a common bath, the collective coordinate  $x$  decomposes into independent mode contributions  $x_i \propto (a_i + a_i^\dagger)$ , and the Hamiltonian becomes identical to the dual-rail form  $H_{SB}^{(\text{DR})}$ . Therefore, the dual-rail model can be viewed as the limiting case of our  $xB$  interaction under the assumptions of the RWA and non-collective decoherence.

Physically, the essential distinction lies in the microscopic origin of the coupling. In the dual-rail scenario, each rail represents a distinguishable physical channel that undergoes its own amplitude damping, so the environment monitors and decoheres the two rails individually. In the present identical-particle framework, the logical qubit is encoded in intrinsic collective degrees of freedom of indistinguishable bosons (such as symmetric or antisymmetric combinations of occupation states), and the bath couples to the total coordinate rather than to individual modes. This collective, symmetry-preserving decoherence does not remove the system from the logical manifold and thus allows a direct recovery process within the same Hilbert space. In summary, the dual-rail encoding describes the regime of independent, distinguishable-mode decoherence, while the present  $xB$ -type Hamiltonian captures the opposite limit of collective coupling among identical particles, which forms the basis for our nonunitary correction scheme.

The fundamental difference between the two schemes also manifests in their capability of error recovery. In the dual-rail encoding, photon loss removes the system from the logical subspace, producing the vacuum state  $|0, 0\rangle$  that carries no logical information. Although such events can be detected through parity or total-photon-number measurements, the logical state cannot be reconstructed without reintroducing a photon from an external source. Therefore, dual-rail architectures are intrinsically limited to error *detection*, and any restoration of the logical state requires a full reinitialization process.

In contrast, the present identical-particle encoding remains within the logical manifold even after environmental coupling. The collective  $xB$  interaction merely distorts the relative amplitudes of the logical basis states while preserving their particle-exchange symmetry. Such errors can be deterministically reversed through a nonunitary inverse operation that rescales the affected amplitudes. This allows genuine error *correction* within the same physical Hilbert space, without resorting to reinitialization or ancilla-mediated recovery. Hence, while dual-rail qubits serve as valuable detectors of photon-loss events, the identical-particle qubit proposed here provides a physically realizable mechanism for restoring logical information under collective decoherence.

### III. EXACT SYSTEM-BATH DYNAMICS

We now turn to the dynamics of the encoded modes coupled to bosonic environments. Our goal is twofold: (i) to obtain closed-form expressions for the Heisenberg evolution of the relevant system operators, which directly determine the reduced dynamics in the encoding subspace, and (ii) to use these expressions to design control protocols that suppress leakage and logical errors. In the main text we present the central results and their physical consequences; detailed derivations are deferred to Appendix B.

#### A. Hamiltonian of the IPQ-boson model

The identical particles forming the IPQ interact with a common bosonic thermal reservoir at a finite inverse temperature  $\beta$ , or couple to their individual bosonic reservoirs at finite temperatures  $T_i$ . The total Hamiltonian is given by

$$H_{\text{tot}} = H_S + H_B + H_{\text{SB}},$$

where  $H_B = \sum_{i,\alpha} \omega_{i,\alpha} b_{i,\alpha}^\dagger b_{i,\alpha}$  represents the reservoir Hamiltonian for individual decoherence, and  $H_B = \sum_{\alpha} \omega_{\alpha} b_{\alpha}^\dagger b_{\alpha}$  describes the collective decoherence reservoir Hamiltonian. The interaction Hamiltonian is

$$H_{\text{SB}} = \sum_i L_i \otimes B_i + \text{h.c.},$$

where  $L_i$  and  $B_i$  are the system and reservoir operators, respectively. Here, we consider the rotating wave approximation for  $H_{\text{SB}}$ .

For collective reservoir coupling, there is only one system operator involved in  $H_{\text{SB}}$ , i.e.,  $L_0 = (c_0 + c_1)/\sqrt{2}$ , with the corresponding reservoir operators given by  $B_0 = \sum_{\alpha} g_{\alpha}^* b_{\alpha}^\dagger$ . In contrast, if the identical particles interact with their reservoirs individually, the interaction Hamiltonian is

$$H_{\text{SB}} = \sum_{i=0,1} c_i \otimes \sum_{\alpha} g_{i,\alpha}^* b_{i,\alpha}^\dagger + \text{h.c.}$$

The IPQ Hamiltonian consists of two parts,  $H_S = H_S^0 + H_C$ , where

$$H_S^0 = \sum_{k=x,z} G_k J_k$$

is the gate operation Hamiltonian, and

$$H_C = \mu(t) \sum_i c_i^\dagger c_i \quad (18)$$

is the LEO Hamiltonian.

#### B. Collective decoherence

In this section, the identical particles couple to a common thermal reservoir, which induces collective decoherence in the IPQ system. To simplify the analysis, we introduce two collective operators:  $a_1 = (c_1 + c_0)/\sqrt{2}$  and  $a_0 = (c_1 - c_0)/\sqrt{2}$ , which satisfy the commutation relation  $[a_i, a_j] = \delta_{ij}$ . In terms of these collective operators, the interaction Hamiltonian becomes

$$H_{\text{SB}} = \sum_{\alpha} g_{\alpha}^* a_1 \otimes b_{\alpha}^\dagger + \text{h.c.},$$

where  $a_1$  interacts with the reservoir modes. The corresponding gate operation operators can be expressed in terms of  $a_i$  as follows

$$J_x = a_1^\dagger a_1 - a_0^\dagger a_0,$$

$$J_z = a_1^\dagger a_0 + a_0^\dagger a_1.$$

Additionally, the LEO Hamiltonian [Eq. (18)] in this representation reads

$$H_C = \mu(t) \sum_{i=0,1} a_i^\dagger a_i.$$

This structure allows for the application of LEO pulses to protect the system from the effects of decoherence.

According to the Heisenberg equation, we can obtain the evolution equation of  $a_i(t)$  in the Heisenberg picture. To obtain the exact dynamics under collective decoherence, we solve the Heisenberg equations of motion for the system operators and eliminate the reservoir modes. The full derivation and the explicit time-dependent coefficients are given in Appendix B. Here we only quote the resulting operator solution,

$$a_i(t) = \sum_{k=0,1} C_i^k(t) a_k(0) + \sum_{\alpha} B_{c,\alpha}^i(t) b_{\alpha}(0), \quad (19)$$

which fully determines all system observables for arbitrary initial system and bath states.

The IPQ-B interaction can be written as  $H_{\text{SB}} = \sum_{\alpha} g_{\alpha} (a_1^\dagger b_{\alpha} + a_0 b_{\alpha}^\dagger)$ , where  $a_1 = (c_1 + c_0)/\sqrt{2}$  and the commuting system operator is  $a_0 = (c_1 - c_0)/\sqrt{2}$ . The system Hamiltonian is given by  $H_S^0 = \sum_{k=0,x,z} G_k J_k$ , with  $G_k$  representing the gate operation strength. Here,  $J_0 = I_2$  denotes a null operator corresponding to the information storage process. The Hamiltonian for the thermal bosonic reservoir is  $H_B = \sum_{\alpha} \omega_{\alpha} b_{\alpha}^\dagger b_{\alpha}$ .

We expand the identical-particle operators at time  $t$  in the initial system/bath modes,

$$c_j(t) = \sum_{i=0,1} C_i^j(t) c_i^0 + \sum_{\alpha} B_{c,\alpha}^j(t) b_{\alpha}^0, \quad (20)$$

In particular, under collective decoherence the shared reservoir induces mode mixing between the two identical-particle modes. For example, setting  $j = 0$  in Eq. (20) gives

$$c_0(t) = C_0^0(t) c_0^0 + C_1^0(t) c_1^0 + \sum_{\alpha} B_{c,\alpha}^0(t) b_{\alpha}^0, \quad (21)$$

so that  $c_0(t)$  generally depends on both  $c_0^0$  and  $c_1^0$ .

and, without additional assumptions (the Appendix treats more general bilinear cases beyond the rotating-wave approximation), derive exact evolution equations for the coefficients. These equations directly yield single- and two-particle observables [35], and the model is analytically solvable [51]. For individual dynamics we evaluate the average excitation  $n_i(t) = c_i^{\dagger}(t) c_i(t)$ ,

$$\langle n_i(t) \rangle = \sum_{j=0,1} |C_j^i(t)|^2 \langle c_j^{0\dagger} c_j^0 \rangle_S + \sum_{\alpha} |B_{c,\alpha}^i(t)|^2 \frac{1}{e^{\beta\omega_{\alpha}} - 1}.$$

As  $t \rightarrow \infty$ ,  $|C_j^i(t)|^2 \rightarrow 0$  and the single particle thermalizes to the bath temperature, consistent with the yellow dotted and purple dot-dashed curves in Fig. 1(a).

To assess gate errors we define the target-IPQ effective state

$$\rho_{\text{eff}} = \frac{1}{2} \left( I_2 + \sum_{k=x,y,z} \langle J_k \rangle \sigma_k \right),$$

obtained by tracing out all non-target qubits from the (possibly entangled) multi-IPQ state at the evaluation time. The effective Bloch components are

$$\langle J_k(t) \rangle = \sum_{i,j=0,1} C_{ij}^k(t) \langle c_i^{0\dagger} c_j^0 \rangle_S + \sum_{\alpha} \mathcal{B}_{\alpha}^k(t) \frac{1}{e^{\beta\omega_{\alpha}} - 1},$$

where  $C_{ij}^k(t)$  and  $\mathcal{B}_{\alpha}^k(t)$  are functions of  $C_i^k(t)$  and  $B_{c,\alpha}^k(t)$  [35]. The first term captures gate-operation, initial-state, and dissipative contributions [52]; the second is the purely thermal contribution (the only part depending on  $1/\beta$ ).

### C. Dynamical decoupling with LEO

We first determine the LEO operator and explore how it dynamically decouple the interaction between the IPQ and bath [30, 53]. By following process in Ref. [30], it is easy to show:  $R_L = R_L^{\dagger} = e^{-i\pi(c_0^{\dagger} c_0 + c_1^{\dagger} c_1)}$ , such that  $R_L H_{SB} R_L = -H_{SB}$  and  $R_L H_a R_L = H_a$ , where  $a = S, B$ . Ideally, by toggling  $R_L$  on and off over a duration of  $2\delta t$ , the entire system evolves as follows:  $e^{-iH\delta t} R_L e^{-iH\delta t} R_L = e^{-2i(H_S + H_B)\delta t}$ , indicating that  $R_L$  acts as an LEO with the corresponding Hamiltonian  $H_{\text{LEO}}(t) = \mu(t) \sum_{i=0}^1 c_i^{\dagger} c_i$  [30, 54].  $\mu(t)$  is an external field on the system, for example, an external magnetic field such that  $\mu_{\text{eff}} = \mu + g\mu_b |B_z|/2$  [55]. By applying a

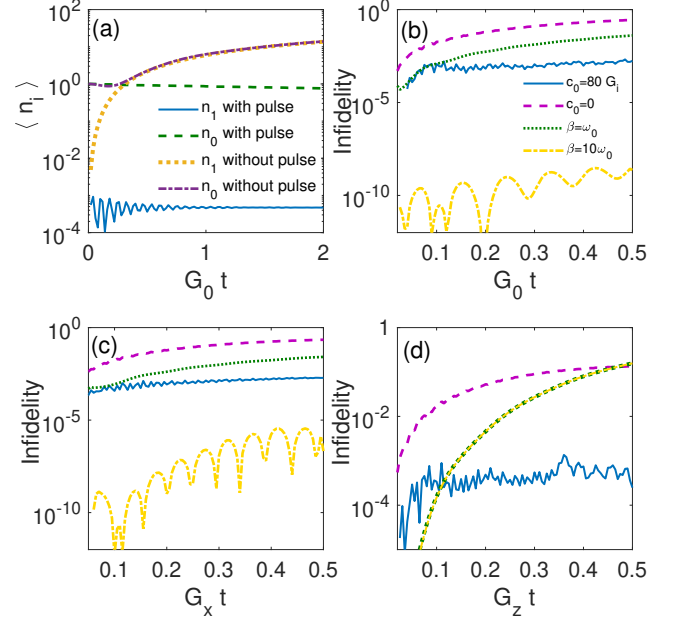


FIG. 1. (a) The evolution of the average excitation number for a single identical particle. (b-d) The infidelity of the effective density matrices during (b) information storage, (c) Z-gate operation, and (d) X-gate operation. The dashed purple lines represent the system without applying LEO pulses, while the blue solid lines show the results with LEO pulses applied. The temperature parameters are set as  $\beta = \omega_0^{-1}$  and  $\Omega = \omega_0$ . The dotted green lines and the yellow dashed-dotted lines correspond to the decoherence-free subspace (DFS) state for  $a_0(t)$  with  $\beta = \omega_0^{-1}$  and  $\beta = 10\omega_0^{-1}$ , respectively. System parameters are chosen as  $\Gamma = 5G_k$ ,  $\gamma = 0.5G_k$ , and  $\omega_0 = 100G_k$ . The LEO pulse parameters are configured with pulse strength  $c_0 = 50G_k$ , pulse width  $\Delta\tau = 0.02\pi G_k^{-1}$ , and pulse spacing  $\delta\tau = 0.005\pi G_k^{-1}$ . The unit  $G_k = 1$ , where  $k = 0, x, z$ , is used for other parameters, with  $G_0 = 1$  for  $H_S^0 = G_0 I_2$ .

time-dependent  $B_z$ , one can achieve a controllable  $\mu_{\text{eff}}$ . It is noteworthy that the LEO is effective for all linear couplings  $H_{SB}$ . Significantly, the LEO Hamiltonian  $H_{\text{LEO}}$  commutes with the set  $\{J_k\}$  and all single- and double-qubit gates, allowing  $R_L$  to be applied independently of these gates as background pulses or noise.

To clarify the mechanism by which LEO pulses suppress decoherence, we focus on the subspace of operators constructed from the initial system annihilation operators  $\{c_0^0, c_1^0\}$ , referred to as *the encoding subspace*. As observed from Eq. (20), if the system is closed, not only will the system annihilation operators at any given time remain within the encoding subspace, but the sum of the squared magnitudes of the expansion coefficients in Eq. (20) will also remain constant. Within this encoding subspace, there are four independent expansion coefficients. We define a vector of coefficients as  $\vec{C}(t) = [C_1^1(t), C_0^1(t), C_1^0(t), C_0^0(t)]^T$ , which encompasses all the relevant components. It has been demonstrated

in the supplementary material that the dynamical equation for  $\vec{C}(t)$ , encompassing all operations executed on the IPQ, can be expressed in a unified form [35]

$$\begin{aligned} \dot{\vec{D}}_k(t) &= -i G_k \bar{\sigma}_z \otimes \bar{I}_2 \vec{D}_k(t) \\ &- \int_0^t ds \exp\left(-i \int_s^t d\tau \mu(\tau)\right) \bar{F}(t-s) \vec{D}_k(t) \end{aligned} \quad (22)$$

where  $\vec{D}_k(t) = \bar{U}_k \vec{C}(t) e^{-i \int_0^t d\tau \mu(\tau)}$  is a slow-varying vector with a diagonalized gate operation matrix  $\bar{\sigma}_z \otimes \bar{I}_2$ . Here,  $k = x, y, 0$  corresponds to the X gate operation, the Z gate operation, and the information storage process (with  $G_0 = 0$ ), respectively. The matrix  $\bar{U}_k$  is a constance. The function  $\bar{F}(t-s)$  represents an integral kernel matrix that includes the correlation functions of the thermal reservoirs [35]. When  $e^{-i \int_s^t \mu(\tau) d\tau}$  represents a fast oscillation term and  $\bar{F}(t-s)$  is a slowly varying matrix, the integral term in Eq. (22) approaches zero according to the Riemann-Lebesgue lemma [56, 57]. As a result, Eq. (22) simplifies to  $\dot{\vec{D}}(t) = -i G_k \bar{\sigma}_z \otimes \bar{I}_2 \vec{D}(t)$ , which corresponds to the ideal  $k$ -gate operation for the IPQ.

Our numerical analysis is shown in FIGs. 1 (a-d), where the system initial state is  $|\psi_0\rangle = \frac{\sqrt{2}}{2}(|1\rangle + |0\rangle)$ . We employ the Lorentzian spectral density given by  $J(\omega) = \frac{\Gamma \gamma^2 / 2\pi}{(\omega - \Omega)^2 + \gamma^2}$  where  $\gamma$  represents the spectral width,  $\Omega$  denotes the central frequency of the reservoir, and  $\Gamma$  is the global dissipation rate. Numerical results further confirm that the application of LEO pulses effectively suppresses single-particle thermalization, allowing the particles to maintain their original quantum states, as shown by the solid blue line and dashed green line in FIG. 1 (a). Then we examine the dynamics of infidelity (error rate) during gate operations. As illustrated by the purple dashed line in FIG. 1 (b-d), the infidelity between  $\rho_{\text{eff}}$  and  $\rho_{\text{eff}}^0$  rapidly increases when LEO pulses are absent, where  $\rho_{\text{eff}}^0$  is the effective density matrix without the IPQ-B interaction. In contrast, when LEO pulses are implemented, the infidelity across various gate operations remains below  $10^{-3}$ , as shown by the solid blue lines in FIG. 1 (b-d).

The collective mode  $a_0(t)$  is invariant because  $[a_0, H_{SB}] = 0$ . The eigenstate of  $a_0^\dagger(0)a_0(0)$ ,  $|\psi_{\text{DFS}}\rangle = \frac{\sqrt{2}}{2}(|1\rangle - |0\rangle)$ , thus forms a decoherence-free subspace (DFS) usable as a special initial state. Without LEO, Fig. 1(b-d) shows green dotted ( $\beta = \omega_0^{-1}$ ) and yellow dot-dashed ( $\beta = 10\omega_0^{-1}$ ) traces: storage and X gates improve at lower temperature, whereas the Z-gate infidelity is essentially temperature-insensitive. With LEO, the Z gate remains high-fidelity and thermal noise is strongly suppressed for all gates. Further derivations and extended scans are given in the Supplemental Material [35].

TABLE II. Error Classification and Comparison

Model	Primary errors	Secondary errors	Pauli errors
Qubit-Boson	$\vec{\sigma} \cdot \vec{B}$	$\vec{\sigma}_i \cdot \mathbf{G}_{ij} \cdot \vec{\sigma}_j$	$\vec{\sigma}$
IPQ-Boson	$(c_0^\dagger + c_1^\dagger)b + h.c.$	$\vec{J} \cdot \vec{B}$	$\vec{J}$

#### D. Two-qubit gate

We consider a two-logical-qubit system composed of two IPQs,  $a^\alpha$  and  $a^\beta$ , where information is encoded in logical qubits as  $|i\rangle_k = a_i^k |\text{vacuum}\rangle$ , with qubit labels  $k = \alpha, \beta$  and state labels  $i = 0, 1$ . A control-phase (C-phase) gate [60] can be implemented using the Hamiltonian  $H_{\text{cp}} = \varepsilon_{\text{cp}} n_0^\alpha n_0^\beta$ , where  $n_0^{\alpha, \beta}$  are particle number operators. The corresponding evolution operator for the C-phase gate is  $U_{\text{cp}} = \exp\left(-i \int_0^\tau \varepsilon_{\text{cp}}(\tau) n_0^\alpha n_0^\beta d\tau\right)$ . Since the coupling only involves the quantum state  $|0\rangle_k$ , we have  $H_{\text{cp}}|1\rangle_k = 0$  for all  $k$ . This implies that the C-phase gate does not induce any phase shift on quantum states containing  $|1\rangle_k$ . When  $H_{\text{cp}}$  acts on  $|0\rangle_\alpha |0\rangle_\beta$ ,  $U_{\text{cp}}$  generates a phase shift of  $\alpha_{\text{cp}} = \int_0^\tau \varepsilon_{\text{cp}}(\tau) d\tau$ , resulting in a C-phase gate when  $\alpha_{\text{cp}} = \pi$ . We designed the C-phase gate in this way because  $H_{\text{cp}}$  commutes perfectly with the LEO Hamiltonian  $H_{\text{LEO}}$ . This ensures that applying LEO pulses to protect the C-phase gate operation does not introduce additional errors, highlighting a key advantage of our proposal in the context of dynamical decoupling. Since the C-phase gate involves only two-body interactions between the identical particles  $a_0^\alpha$  and  $a_0^\beta$ , the coupling strength  $\varepsilon_{\text{cp}}$  should be comparable to that of single-qubit gate operations. As shown in our numerical results for the single gate operations, even when the gate operation strength is much lower than the particle-system coupling strength, high fidelity can still be achieved with LEO pulse application. Thus, our proposal demonstrates excellent robustness.

Physically, interactions between different optical wells in cold atom optical lattices can be achieved by tuning atomic contact interactions or long-range dipole-dipole interactions. These are typically controlled by adjusting the atomic scattering length or using Feshbach resonances [64]. In circuit quantum electrodynamics (cQED) systems, two superconducting resonators or qubits can interact through shared nonlinear elements, like Josephson junctions, leading to an interaction Hamiltonian of the form  $H_{\text{cp}}$  [65]. Kerr nonlinearities or cross-mode coupling are common ways to realize these interactions [66]. Additionally, in cQED, dispersive coupling under far-detuned conditions enables interactions between qubits and cavity modes that generate frequency shifts based on particle number, resulting in an effective  $H_{\text{cp}}$  interaction [67].

#### IV. INDIVIDUAL DECOHERENCE

The analysis above assumes a collective reservoir that couples to both modes and can mediate correlated noise. Many platforms, however, are better described by independent reservoirs acting on each mode. In this section we summarize the main dynamical consequences of such individual decoherence and present numerical results that highlight regimes where thermal noise can be strongly suppressed. Technical derivations are collected in Appendix C.

Although collective decoherence dominates, individual decoherence cannot be entirely disregarded. We now consider the process of individual decoherence. When two bosons interact separately with their individual bosonic thermal reservoirs, the dynamics of the identical particle qubit differ significantly from those under collective decoherence. In this scenario, we examine the case where the two bosonic thermal reservoirs have similar spectrum density but are independent, with potentially differing temperatures.

Unlike the collective decoherence, here we consider the total Hamiltonian without the rotating wave approximation. The identical particles that construct the IPQ couple to their own bosonic reservoirs at finite reservoir temperatures  $\beta_i$  individually. The total Hamiltonian is

$$H_{\text{tot}} = H_S + H_B + H_{SB},$$

where  $H_B = \sum_{i,\alpha} \omega_{i,\alpha} b_{i,\alpha}^\dagger b_{i,\alpha}$  is the reservoir Hamiltonian and

$$H_{SB} = \sum_{i=0,1} (c_i^\dagger + c_i) \sum_{\alpha} g_{i,\alpha} (b_{i,\alpha}^\dagger + b_{i,\alpha})$$

with the coupling strengths  $g_{i,\alpha}$ . The IPQ Hamiltonian contains two parts,

$$H_S = H_S^0 + H_C,$$

where  $H_S^0 = \sum_i \omega_{0,i} c_i^\dagger c_i + \sum_{K=x,z} G_k J_K$  is the free Hamiltonian and the gate Hamiltonian, and  $H_C = \mu(t) \sum_i c_i^\dagger c_i$  is the LEO Hamiltonian.

##### A. Model and main results

Starting from the total Hamiltonian above and eliminating the independent reservoirs, the exact non-Markovian evolution can be written in a linear form in terms of the initial system and bath operators,

$$\begin{aligned} c_j(t) &= \sum_{i=0,1} \left( C_i^j(t) c_i^0 + \bar{C}_i^j(t) c_i^{0\dagger} \right) \\ &\quad + \sum_{i,\alpha} \left( B_{i,\alpha}^j(t) b_{i,\alpha}^0 + \bar{B}_{i,\alpha}^j(t) b_{i,\alpha}^{0\dagger} \right), \\ c_j^\dagger(t) &= \sum_{i=0,1} \left( C_i^{j*}(t) c_i^{0\dagger} + \bar{C}_i^{j*}(t) c_i^0 \right) \\ &\quad + \sum_{i,\alpha} \left( B_{i,\alpha}^{j*}(t) b_{i,\alpha}^{0\dagger} + \bar{B}_{i,\alpha}^{j*}(t) b_{i,\alpha}^0 \right), \end{aligned}$$

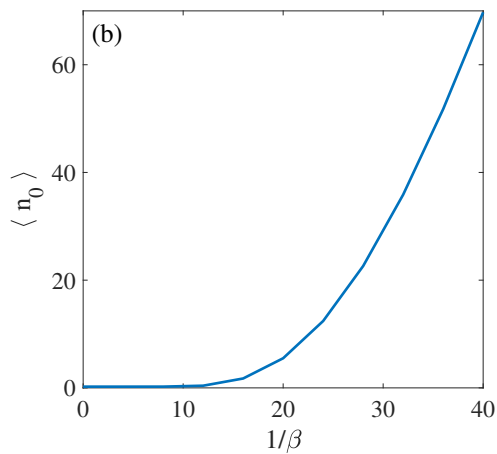
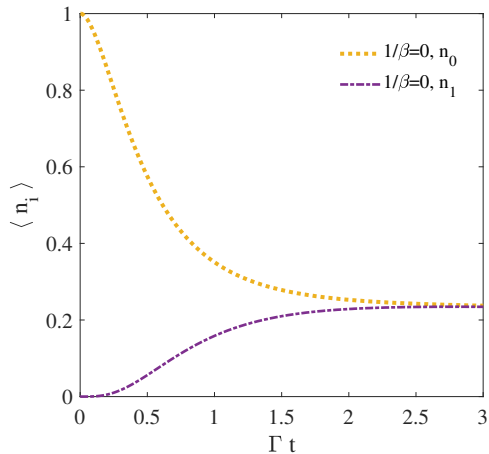


FIG. 2. (a) The average excitation number as a function of dimensionless time  $\Gamma t$ . (b) The steady state average excitation number as a function of  $1/\beta$ . The system parameters are set to  $\gamma = 2.5\Gamma$ , and  $\omega_0 = 100\Gamma$ . No gate operation is used. All other parameters use  $\Gamma = 1$ .

where we have used the definitions  $c_i^0 \equiv c_i(0)$  and  $b_{i,\alpha}^0 \equiv b_{i,\alpha}(0)$ .

For later use, it is convenient to note that, in the absence of direct mode-mode coupling (e.g., during information storage with  $G_x = G_z = 0$ ), the individual-reservoir structure implies that each mode couples only to its own bath. In particular,

$$\begin{aligned} c_0(t) &= C_0^0(t) c_0^0 + \bar{C}_0^0(t) c_0^{0\dagger} \\ &\quad + \sum_{\alpha} \left( B_{0,\alpha}^0(t) b_{0,\alpha}^0 + \bar{B}_{0,\alpha}^0(t) b_{0,\alpha}^{0\dagger} \right), \end{aligned} \quad (23)$$

and analogously for  $c_1(t)$  with the replacement  $0 \rightarrow 1$ . This absence of reservoir-mediated cross terms is the key ingredient behind the thermal-noise cancellation discussed below. Detailed derivations are provided in Appendix C.

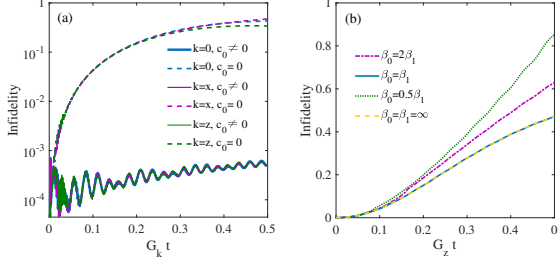


FIG. 3. The infidelity as a function of dimensionless time  $G_k t$ . (a) Infidelity for different gate operations with  $\beta_1 = \beta_2 = 0.1\omega_0^{-1}$ . (b) Infidelity for varying reservoir temperature differences without applying LEO pulses. The system parameters are set to  $\Gamma = 5G_k$ ,  $\gamma = 0.5G_k$ , and  $\omega_0 = 100G_k$ . The LEO pulse parameters include pulse strength  $c_0 = 80G_k$ , pulse width  $\Delta\tau = \pi/50G_k$ , and pulse spacing  $\delta\tau = \pi/200G_k$ . All other parameters use  $G_k = 1$ , with  $k = 0, x, z$ .

## B. Numerical results

First, we consider the time evolution of the average excitation number of a single identical particle in the absence of gate operations, as shown in Fig. 2 (a). We assume that initially a single excitation occupies mode 0, i.e.,  $|0\rangle = c_0^\dagger|\text{vacuum}\rangle$ . When the environment is at zero temperature (yellow dotted and purple dash-dotted lines), the excitations in the two modes tend toward equilibrium. Unlike the case of independent decoherence, the steady state under collective decoherence does not correspond to zero excitation number. This is because the common environment induces an effective indirect interaction between the two modes. As the environmental temperature increases, the average excitation number in each mode also increases [see Fig. 2 (b)]. Therefore, the inclusion of all error channels in the leading-order interaction is physically well justified.

As shown in Fig. 3 (a), the LEO method continues to perform exceptionally well in protecting gate operations. In contrast, when LEO pulses are not applied, the optimal fidelity is achieved at zero temperature difference, regardless of the environmental temperature, as confirmed by Fig. 3 (b). Additionally, we observe that at any temperature, as long as the two thermal reservoirs have no temperature difference, fidelity remains unchanged. This indicates that under zero temperature difference conditions, both information storage and Z-gate operations are free from thermal noise. To make this cancellation transparent, we quote the analytic expressions for the effective Bloch components (derived in Appendix C). In the con-

tinuous limit one finds

$$\begin{aligned} \langle J_z(t) \rangle &= \sum_{i,j=0}^1 (C_j^{1*}(t)C_i^1(t) - C_j^{0*}(t)C_i^0(t)) \langle c_j^{0\dagger}c_i^0 \rangle_S \\ &+ \int d\omega J_1(\omega) \mathcal{B}_1(\omega) \frac{1}{e^{\beta_1\omega} - 1} \\ &- \int d\omega J_0(\omega) \mathcal{B}_0(\omega) \frac{1}{e^{\beta_0\omega} - 1}, \end{aligned} \quad (24)$$

and

$$\begin{aligned} \langle J_x(t) \rangle &= \sum_{i,j=0}^1 (C_i^{1*}(t)C_j^0(t) + C_i^{0*}(t)C_j^1(t)) \langle c_i^{0\dagger}c_j^0 \rangle_S, \\ \langle J_y(t) \rangle &= \sum_{i,j=0}^1 i (C_i^{1*}(t)C_j^0(t) - C_i^{0*}(t)C_j^1(t)) \langle c_i^{0\dagger}c_j^0 \rangle_S \end{aligned} \quad (25)$$

This observation can be explained by Eqs. (24) and (25). Specifically, the x- and y-components of the Bloch vector are independent of the reservoir temperatures. When the two bosonic thermal reservoirs have the same temperature, the thermal noise contributions to the z-component cancel each other out.

From a physical perspective, the absence of thermal noise is caused by the interaction with individual reservoirs. When the IPQ interacts with a common thermal reservoir, the shared environment induces indirect coupling between the identical particles, causing  $c_0(t)$  to depend not only on the expansion coefficients of  $c_0^0$ , but also on those of  $c_1^0$  [see Eq.(21)]. In contrast, when identical particles interact with their own thermal reservoirs,  $c_0(t)$  is expanded only in terms of  $c_0$ , isolating the transitions between the identical particles [see Eq.(23)]. When the thermal noise effects are identical, they cancel each other out, rendering the system's dynamics unaffected by environmental temperature. As shown in Fig. 3 (a), under the influence of LEO pulses, the impact of thermal noise is significantly suppressed across all gate operations.

## V. CONCLUSION

We have shown that the first-order system-bath interaction in our identical particle qubit scheme differs fundamentally from conventional first-order qubit-bath interactions, as illustrated in Table II. This new observation requires a reconstruction of traditional strategies to fight decoherence, such as QECC, DD, and DFS, while retaining the foundational principles. Remarkably, we demonstrate that these strategies can be unified into a single code, specifically an unconventional quantum error-correcting code, provided that conventional recovery procedures are generalized beyond unitary operations to include physically implementable reversal operations, thereby placing physical and logical qubits on equal footing. We also notice that the Stabilizer generator aligning with LEO and one of the IPQ states forming a DFS. Interestingly the LEO in our framework also

applies to conventional qubit-bath interactions. Moreover, well-established quantum error correction (QEC) schemes must be reactivated when these second-order IPQ-B interactions in Table II become comparatively significant. The analytically solvable IPQ-B interaction also allows precise validation of existing protocols to fight decoherence, in particular numerical demonstrations of LEO's effectiveness.

### ACKNOWLEDGMENTS

This work was supported by the National Natural Science Foundation of China (NSFC) under Grants Nos. 12205037, 12375009, 12075050 and 12574384; by the Liaoning Provincial Science and Technology

Joint Program (Key Research and Development Program Project) under Grant No. 2025JH2/101800316; by the Fundamental Research Funds for the Central Universities under Grant No. 044420250075; by the grant PID2021-126273NB-I00 funded by MCIN/AEI/10.13039/501100011033, and by *ERDF A way of making Europe* and the Basque Government through Grant No. IT1470-22. This work has been financially supported by the Ministry for Digital Transformation and of Civil Service of the Spanish Government through the QUANTUM ENIA project call-Quantum Spain project, and by the European Union through the Recovery, Transformation and Resilience Plan-NextGenerationEU within the framework of the Digital Spain 2026 Agenda. L.-A.W. thanks Prof. D. Lidar for early communication on this paper.

### Appendix A: Commutation relations of the single-qubit generators

The single qubit gate operations are defined as

$$\begin{aligned} J_x &= c_0 c_1^\dagger + c_0^\dagger c_1, \\ J_y &= i \left( c_0^\dagger c_1 - c_0 c_1^\dagger \right), \\ J_z &= c_1^\dagger c_1 - c_0^\dagger c_0. \end{aligned}$$

The commutation relations between the gate operations read

$$\begin{aligned} [J_x, J_z] &= \left[ c_0 c_1^\dagger + c_0^\dagger c_1, c_1^\dagger c_1 - c_0^\dagger c_0 \right] \\ &= \left[ c_0 c_1^\dagger, c_1^\dagger c_1 \right] + \left[ c_0^\dagger c_1, c_1^\dagger c_1 \right] - \left[ c_0 c_1^\dagger, c_0^\dagger c_0 \right] - \left[ c_0^\dagger c_1, c_0^\dagger c_0 \right] \\ &= -c_0 c_1^\dagger + c_0^\dagger c_1 - c_1^\dagger c_0 + c_1 c_0^\dagger \\ &= -2i \left( i \left( c_0^\dagger c_1 - c_0 c_1^\dagger \right) \right) \\ &= -2i J_y, \end{aligned}$$

$$\begin{aligned} [J_x, J_y] &= i \left[ c_0 c_1^\dagger + c_0^\dagger c_1, c_0^\dagger c_1 - c_0 c_1^\dagger \right] \\ &= i \left( \left[ c_0 c_1^\dagger, c_0^\dagger c_1 \right] - \left[ c_0^\dagger c_1, c_0 c_1^\dagger \right] \right) \\ &= 2i \left( c_0 c_0^\dagger c_1^\dagger c_1 - c_0^\dagger c_0 c_1 c_1^\dagger \right) \\ &= 2i \left( c_1^\dagger c_1 + c_0^\dagger c_0 \left( c_1^\dagger c_1 - c_1 c_1^\dagger \right) \right) \\ &= 2i \left( c_1^\dagger c_1 - c_0^\dagger c_0 \right) \\ &= 2i J_z. \end{aligned}$$

The communication relations between LEO Hamiltonian and gate operations fulfill

$$\begin{aligned}
[H_C, J_x] &= \mu \left[ c_0 c_0^\dagger + c_1^\dagger c_1, c_0 c_1^\dagger + c_0^\dagger c_1 \right] \\
&= \mu \left( \left[ c_0 c_0^\dagger, c_0 \right] c_1^\dagger + \left[ c_0 c_0^\dagger, c_0^\dagger \right] c_1 + \left[ c_1^\dagger c_1, c_1^\dagger \right] c_0 + \left[ c_1^\dagger c_1, c_1 \right] c_0^\dagger \right) \\
&= \mu \left( -c_0 c_1^\dagger + c_0^\dagger c_1 + c_1^\dagger c_0 - c_1 c_0^\dagger \right) \\
&= 0, \\
[H_C, J_y] &= i\mu \left[ c_0 c_0^\dagger + c_1^\dagger c_1, c_0^\dagger c_1 - c_0 c_1^\dagger \right] \\
&= i\mu \left( \left[ c_0 c_0^\dagger, c_0^\dagger \right] c_1 - \left[ c_0 c_0^\dagger, c_0 \right] c_1^\dagger + \left[ c_1^\dagger c_1, c_1 \right] c_0^\dagger - \left[ c_1^\dagger c_1, c_1^\dagger \right] c_0 \right) \\
&= i\mu \left( c_0^\dagger c_1 + c_0 c_1^\dagger - c_1^\dagger c_0 - c_1 c_0^\dagger \right) \\
&= 0, \\
[H_C, J_z] &= i\mu \left[ c_0 c_0^\dagger + c_1^\dagger c_1, c_1^\dagger c_1 - c_0^\dagger c_0 \right] \\
&= 0, \\
[H_C, H_{\text{cp}}] &= i\varepsilon_{\text{cp}} \left[ c_0 c_0^\dagger + c_1^\dagger c_1, c_1^\dagger c_1 c_0^\dagger c_0 \right] \\
&= 0.
\end{aligned}$$

## Appendix B: Collective decoherence: derivations

### 1. Dynamics in the encoding subspace (collective reservoir)

We encode the information in the operator subspace spanned by  $\{c_i^0, c_i^{0\dagger}\}$ . Decoherence causes information to leak from this subspace, leading to failures in both information storage and gate operations. First, we examine the dynamics of the encoding subspace in the  $a_i$  representation. Specifically, we focus on the coefficients  $A_i^0$  and  $A_i^1$ , whose evolution is governed by the following equations:

$$\dot{A}_0^0(t) = -i(\mu(t) - G_x) A_0^0(t) - i G_z A_0^1(t), \quad (\text{B1})$$

$$\dot{A}_1^0(t) = -i(\mu(t) - G_x) A_1^0(t) - i G_z A_1^1(t) \quad (\text{B2})$$

$$\dot{A}_0^1(t) = -i(\mu(t) + G_x) A_0^1(t) - i G_z A_0^0(t) - \int_0^t ds f(t-s) A_0^1(s), \quad (\text{B3})$$

$$\dot{A}_1^1(t) = -i(\mu(t) + G_x) A_1^1(t) - i G_z A_1^0(t) - \int_0^t ds f(t-s) A_1^1(s). \quad (\text{B4})$$

In what follows, we consider three different gate operations: information storage, X-gate operation and Z-gate operation.

#### a. Information Storage.

In this case, no gate operation is applied, i.e.,  $G_x = G_z = 0$ . The information is encoded in the operator subspace with the basis  $\{a_i^0\}$  at the initial moment, meaning  $A_0^0(0) = A_1^1(0) = 1$  and  $A_0^1(0) = A_1^0(0) = 0$ . At this point, the evolutions of  $A_i^j(t)$  are decoupled from each other:

$$\begin{aligned}
\dot{A}_0^0(t) &= -i\mu(t)A_0^0(t), \\
\dot{A}_1^0(t) &= -i\mu(t)A_1^0(t), \\
\dot{A}_0^1(t) &= -i\mu(t)A_0^1(t) - \int_0^t ds f(t-s) A_0^1(s), \\
\dot{A}_1^1(t) &= -i\mu(t)A_1^1(t) - \int_0^t ds f(t-s) A_1^1(s).
\end{aligned}$$

Introducing slow variants  $\tilde{A}_i^j(t) = A_i^j(t) \exp(-i \int_0^t d\tau \mu(\tau))$ , we have

$$\dot{\tilde{A}}_i^0(t) = 0,$$

$$\dot{\tilde{A}}_i^1(t) = -\exp\left(-i \int_0^t d\tau \mu(\tau)\right) \int_0^t ds f(t-s) \exp\left(i \int_0^s d\tau \mu(\tau)\right) \tilde{A}_i^j(s).$$

As a result, the information encoded in the operator subspace is robust to against collective noise at a finite reservoir temperature. We can rewrite it into a vector equation as

$$\dot{\tilde{\vec{A}}}(t) = -\exp\left(-i \int_0^t d\tau \mu(\tau)\right) \int_0^t ds \bar{f}(t-s) \exp\left(i \int_0^s d\tau \mu(\tau)\right) \tilde{\vec{A}}(s) \quad (\text{B5})$$

with  $\tilde{\vec{A}}(t) = [\tilde{A}_1^1(t), \tilde{A}_0^1(t), \tilde{A}_1^0(t), \tilde{A}_0^0(t)]$ , and

$$\bar{f} = \text{diag}(f, f, 0, 0).$$

*b. The X-Gate operation.*

When we consider a X-gate operation on the IPQ, it requires  $G_z = 0$ , which leads to

$$\begin{aligned} \dot{A}_0^0(t) &= -i(\mu(t) - G_x) A_0^0(t), \\ \dot{A}_1^0(t) &= -i(\mu(t) - G_x) A_1^0(t), \\ \dot{A}_0^1(t) &= -i(\mu(t) + G_x) A_0^1(t) - \int_0^t ds f(t-s) A_0^1(s), \\ \dot{A}_1^1(t) &= -i(\mu(t) + G_x) A_1^1(t) - \int_0^t ds f(t-s) A_1^1(s). \end{aligned}$$

Similar to information storage, the information is encoded in the encoding subspace with the basis  $\{a_i^0\}$ . We introduce  $\tilde{A}_i^j(t)$ , which has the same definition as before. We have

$$\begin{aligned} \dot{\tilde{A}}_i^0(t) &= i G_x \tilde{A}_i^0(t), \\ \dot{\tilde{A}}_i^1(t) &= -i G_x \tilde{A}_i^1(t) - \exp\left(-i \int_0^t d\tau \mu(\tau)\right) \int_0^t ds f(t-s) \exp\left(i \int_0^s d\tau \mu(\tau)\right) \tilde{A}_i^1(s), \end{aligned}$$

which can be written as a vector form

$$\dot{\tilde{\vec{A}}}(t) = -i G_x \bar{\sigma}_z \otimes \bar{I}_2 \tilde{\vec{A}}(t) - \exp\left(-i \int_0^t d\tau \mu(\tau)\right) \int_0^t ds \exp\left(i \int_0^s d\tau \mu(\tau)\right) \bar{f}(t-s) \tilde{\vec{A}}(s),$$

with same variants used in Eq.(B5). Due to rapid oscillation terms in the convolution, the second term in above equations have no contribution on the X-gate operation. Therefore, the effective dynamics will be described by

$$\dot{\tilde{\vec{A}}}(t) = -i G_x \bar{\sigma}_z \otimes \bar{I}_2 \tilde{\vec{A}}(t)$$

with  $\tilde{\vec{A}}(t) = [\tilde{A}_1^1(t), \tilde{A}_0^1(t), \tilde{A}_1^0(t), \tilde{A}_0^0(t)]$ , which is perfect X-gate operation on the IPQ without the decoherence effect.

*c. The Z-Gate Operation.*

Finally, we consider the Z-gate operation with  $G_x = 0$ . As the information needs to be transferred between  $a_0^0$  and  $a_1^0$ , all expansion coefficients of  $a_0^0$  and  $a_1^0$  must be accounted for, with their dynamics described by Eqs. (B1 - B4).

Then we can write down

$$\begin{aligned}\dot{A}_0^0(t) &= -i\mu(t)A_0^0(t) - iG_z A_0^1(t), \\ \dot{A}_1^0(t) &= -i\mu(t)A_1^0(t) - iG_z A_1^1(t), \\ \dot{A}_0^1(t) &= -i\mu(t)A_0^1(t) - iG_z A_0^0(t) - \int_0^t ds f(t-s) A_0^1(t), \\ \dot{A}_1^1(t) &= -i\mu(t)A_1^1(t) - iG_z A_1^0(t) - \int_0^t ds f(t-s) A_1^1(t).\end{aligned}$$

We can rewrite the equations into a vector equation,

$$i\vec{A}(t) = (\mu(t)\bar{I}_4 + G_z\bar{\sigma}_x \otimes \bar{I}_2) \vec{A}(t) + \int_0^t ds \bar{f}(t-s) \vec{A}(s).$$

By using unitary matrix

$$\bar{U}_Z = \frac{\sqrt{2}}{2} \begin{pmatrix} 1 & 0 & -1 & 0 \\ 0 & 1 & 0 & -1 \\ 1 & 0 & 1 & 0 \\ 0 & 1 & 0 & 1 \end{pmatrix},$$

the vector equation can be transformed into

$$\dot{\vec{D}}(t) = -i(\mu(t)\bar{I}_4 + G_z\bar{\sigma}_z \otimes \bar{I}_2) \vec{D}(t) - \int_0^t ds \bar{F}(t-s) \vec{D}(s)$$

with  $\vec{D}(t) = \bar{U}_Z \vec{A}$  and

$$\bar{F} = \bar{U}_Z \bar{f} \bar{U}_Z^\dagger = \frac{1}{2} \begin{pmatrix} f & 0 & -f & 0 \\ 0 & f & 0 & -f \\ -f & 0 & f & 0 \\ 0 & -f & 0 & f \end{pmatrix}$$

By defining  $\tilde{\vec{D}}(t) = \vec{D}(t) \exp(-i \int_0^t d\tau \mu(\tau))$ , we arrive at

$$\begin{aligned}\dot{\tilde{\vec{D}}}(t) &= -iG_z\bar{\sigma}_z \otimes \bar{I}_2 \tilde{\vec{D}}(t) \\ &\quad - \exp\left(-i \int_0^t d\tau \mu(\tau)\right) \int_0^t ds \exp\left(i \int_0^s d\tau \mu(\tau)\right) \bar{F}(t-s) \tilde{\vec{D}}(s).\end{aligned}$$

Due to rapid oscillation caused by  $\exp(\pm i \int_0^s d\tau \mu(\tau))$ , the last term of  $\dot{\tilde{\vec{D}}}(t)$  are canceled in the evolution. Thus we have a more concise effective form:

$$\dot{\tilde{\vec{D}}}(t) = -iG_z\bar{\sigma}_z \otimes \bar{I}_2 \tilde{\vec{D}}(t).$$

When we transform variants  $\vec{D}$  back into  $\vec{A} = U_D^\dagger \vec{D}$ , we obtain a perfect Z-gate operation as

$$\vec{A}(t) = -iG_z\bar{\sigma}_x \otimes \bar{I}_2 \vec{A}(t).$$

The coefficient vector can be transformed from the  $\{a_i\}$  representation to the  $\{c_i\}$  representation by means of a constant unitary matrix:

$$\bar{U}_A = \frac{1}{2} \begin{pmatrix} 1 & 1 & 1 & 1 \\ 1 & 1 & -1 & -1 \\ 1 & -1 & 1 & -1 \\ 1 & -1 & -1 & 1 \end{pmatrix},$$

which leads to  $\vec{C}(t) = \bar{U}_A \vec{A}(t)$ . The gate operation matrices in the  $\{c_i\}$  representation satisfy  $\bar{\sigma}_x \otimes \bar{I}_2 = \bar{U}_A \bar{\sigma}_z \otimes \bar{I}_2 \bar{U}_A^\dagger$  and  $\bar{\sigma}_z \otimes \bar{I}_2 = \bar{U}_A \bar{\sigma}_x \otimes \bar{I}_2 \bar{U}_A^\dagger$ . The correlation function matrix is given by  $\bar{F}_C(t-s) = \bar{U}_A \bar{F}(t-s) \bar{U}_A^\dagger$ . Since  $\bar{U}_A$  is a constant matrix, the action of LEO pulses remains effective. As a result, we can obtain the dynamical equations for the encoding subspace in the  $\{c_i\}$  representation.

## 2. Gate-operation dynamics

To characterize the decoherence dynamics of a single identical particle, we examine the time evolution of the average excitation number  $\langle n_i \rangle$  for the  $i$ th identical particle. We assume that, initially, the system and the heat reservoirs are uncorrelated, with the total density matrix expressed as  $\rho_{\text{tot}} = \rho_S(0) \otimes \rho_B(0)$ . The reservoir is prepared in a thermal equilibrium state:

$$\rho_B(0) = \sum_{n,\alpha} \frac{e^{-\beta\omega_\alpha}}{1 - e^{-\beta\omega_\alpha}} |n_\alpha\rangle \langle n_\alpha|,$$

where  $\beta$  is the inverse reservoir temperature, and  $|n_\alpha\rangle$  is the Fock state with excitation number  $n_\alpha$ . Thus, we have

$$\langle n_i(t) \rangle = \langle c_i^\dagger(t) c_i(t) \rangle = \sum_{j,k=0,1} C_j^{i*}(t) C_k^i(t) \langle c_j^{0\dagger} c_k^0 \rangle_S + \sum_\alpha |B_{c,\alpha}^i(t)|^2 \langle b_\alpha^{0\dagger} b_\alpha^0 \rangle_B,$$

where  $\text{Tr}_B\{b_\beta^{0\dagger} b_\alpha^0 \rho_B(0)\} = \delta_{\alpha\beta}$  has been taken into account.

### a. The X-gate operation.

In what follows, we simulate the average values of the observable variables  $\langle J_x(t) \rangle$ ,  $\langle J_y(t) \rangle$ , and  $\langle J_z(t) \rangle$ , where  $\langle J_k(t) \rangle = \text{Tr}\{J_k(t)\rho_{\text{tot}}\}$ . We consider the expected values of the "Pauli operators" during the X-gate operation. The x-component is

$$\begin{aligned} \langle J_x(t) \rangle &= \langle a_1^\dagger(t) a_1(t) - a_0^\dagger(t) a_0(t) \rangle \\ &= \sum_{i,j=0,1} (A_j^{1*}(t) A_i^1(t) - A_j^{0*}(t) A_i^0(t)) \langle a_j^{0\dagger} a_i^0 \rangle_S \\ &\quad + \sum_{\alpha,\beta} (B_\beta^{1*}(t) B_\alpha^1(t) - B_\beta^{0*}(t) B_\alpha^0(t)) \langle b_\beta^{0\dagger} b_\alpha^0 \rangle_B \\ &= \sum_{i,j=0,1} (A_j^{1*}(t) A_i^1(t) - A_j^{0*}(t) A_i^0(t)) \langle a_j^{0\dagger} a_i^0 \rangle_S \\ &\quad + \sum_\alpha (|B_\alpha^1(t)|^2 - |B_\alpha^0(t)|^2) \langle b_\alpha^{0\dagger} b_\alpha^0 \rangle_B. \end{aligned}$$

We can calculate  $B_\beta^i$  by means of the Laplace transform. Since  $a_0(t)$  decouples to the reservoir, we have  $B_\alpha^0(t) = 0$ . The remaining coefficient obeys

$$\dot{B}_\alpha^1(t) = -i(\mu + G_x) B_\alpha^1(t) - \int_0^t ds f(t-s) B_\alpha^1(s) - i g_\alpha \exp(-i\omega_\alpha t), \quad (\text{B6})$$

where  $f(t-s)$  is the bath correlation function. Performing the Laplace transformation of Eq. (B6), we have

$$\tilde{B}_\alpha^1(t_1) = \frac{-i g_\alpha}{(t_1 + i\omega_\alpha) (t_1 + \tilde{f}(t_1) + i(\mu + G_x))},$$

where  $\tilde{f}(t_1)$  are the Laplace transformation of the correlation function for the reservoir, and  $B_\alpha^1(0) = 0$  are considered. If the correlation function  $f(t-s)$  is given, the solution of can be obtained by taking the inverse Laplace transformation on  $\tilde{B}_\alpha^1(t_1)$ , i.e.,  $B_\beta^1(t) = \mathcal{L}^{-1}[\tilde{B}_\alpha^1(t_1)]$ . By introducing

$$\tilde{B}'_\alpha^1(t_1) = \frac{1}{(t_1 + i\omega_\alpha) (t_1 + \tilde{f}(t_1) + i(\mu + G_x))},$$

we can see that  $B_\beta^1(t) = -ig_\alpha B_\beta^{\prime 1}(t)$  with  $B_\beta^{\prime 1}(t) = \mathcal{L}^{-1}[\tilde{B}_\alpha^{\prime 1}(t_1)]$ , which leads to

$$\begin{aligned}
\langle J_x(t) \rangle &= \sum_{i,j=0,1} (A_j^{1*}(t)A_i^1(t) - A_j^{0*}(t)A_i^0(t)) \langle a_j^{0\dagger} a_i^0 \rangle_S \\
&\quad + \sum_{i,\alpha} |g_\alpha|^2 |B_\alpha^{\prime 1}(t)|^2 \langle b_\alpha^{0\dagger} b_\alpha^0 \rangle_B \\
&= \sum_{i,j=0,1} (A_j^{1*}(t)A_i^1(t) - A_j^{0*}(t)A_i^0(t)) \langle a_j^{0\dagger} a_i^0 \rangle_S \\
&\quad + \sum_{\alpha} |g_\alpha|^2 |B_\alpha^{\prime 1}(t)|^2 \frac{1}{e^{\beta\omega_\alpha} - 1} \\
&= \sum_{i,j=0,1} (A_j^{1*}(t)A_i^1(t) - A_j^{0*}(t)A_i^0(t)) \langle a_j^{0\dagger} a_i^0 \rangle_S \\
&\quad + \int d\omega J(\omega) \mathcal{B}_1(\omega) \frac{1}{e^{\beta\omega} - 1}.
\end{aligned}$$

Here, we have considered the continuous limit of the reservoir modes, i.e.,  $\sum_{\alpha} |g_\alpha|^2 |B_\alpha^{\prime 1}(t)|^2 \rightarrow \int d\omega J(\omega) \mathcal{B}_1(\omega)$ . With a similar procedure,  $\langle J_z(t) \rangle$  and  $\langle J_y(t) \rangle$  are given by

$$\begin{aligned}
\langle J_z(t) \rangle &= \sum_{i,j=0,1} (A_i^{1*}(t)A_j^0(t) + A_i^{0*}(t)A_j^1(t)) \langle a_i^{0\dagger} a_j^0 \rangle_S, \\
\langle J_y(t) \rangle &= \sum_{i,j=0,1} i (A_i^{1*}(t)A_j^0(t) - A_i^{0*}(t)A_j^1(t)) \langle a_i^{0\dagger} a_j^0 \rangle_S,
\end{aligned}$$

where  $B_\alpha^0(t) = 0$  and  $\langle b_\beta^{0\dagger} b_\alpha^0 \rangle_B = \delta_{\alpha\beta} \frac{1}{e^{\beta\omega_\alpha} - 1}$  have been used.

#### b. The Z-gate operation.

The dynamical equations of  $B_\alpha^i(t)$  read

$$\begin{aligned}
\dot{B}_\alpha^0(t) &= -i\mu B_\alpha^0(t) - iG_z B_\alpha^1(t), \\
\dot{B}_\alpha^1(t) &= -i\mu B_\alpha^1(t) - iG_z B_\alpha^0(t) - \int_0^t ds f(t-s) B_\alpha^1(s), \\
&\quad -i g_\alpha \exp(-i\omega_\alpha t),
\end{aligned}$$

We can solve it by the Laplace transformation, which leads to

$$\begin{aligned}
\tilde{B}_\alpha^0(t_1) &= \frac{g_\alpha G_z}{(t_1 + i\omega_\alpha) \left( G_z^2 + (t_1 + i\mu) (t_1 + i\mu + \tilde{f}(t_1)) \right)}, \\
\tilde{B}_\alpha^1(t_1) &= \frac{g_\alpha (t_1 + i\mu)}{(t_1 + i\omega_\alpha) \left( G_z^2 + (t_1 + i\mu) (t_1 + i\mu + \tilde{f}(t_1)) \right)}.
\end{aligned}$$

where  $\tilde{f}_k(t_1) = \mathcal{L}[f_k(t)]$  is the result of the Laplace transformation about  $f_k(t)$ , and  $B_j^i(0) = 0$  is used. If  $f_k(t)$  is given, we can obtain the solutions by means of the inverse Laplace transformation. The mean values of  $\{J_z\}$  read

$$\begin{aligned}
\langle J_z(t) \rangle &= \sum_{i,j=0,1} (A_i^{1*}(t)A_j^0(t) + A_i^{0*}(t)A_j^1(t)) \langle a_i^{0\dagger} a_j^0 \rangle_S \\
&\quad + \sum_{i,\alpha} |g_\alpha|^2 \left( B_\alpha^{\prime 0*}(t) B_\alpha^{\prime 1}(t) + B_\alpha^{\prime 1*}(t) B_\alpha^{\prime 0}(t) \right) \frac{1}{e^{\beta\omega_\alpha} - 1}, \\
\langle J_y(t) \rangle &= \sum_{i,j=0,1} i (A_i^{1*}(t)A_j^0(t) - A_i^{0*}(t)A_j^1(t)) \langle a_i^{0\dagger} a_j^0 \rangle_S \\
&\quad + \sum_{i,\alpha} i |g_\alpha|^2 \left( B_\alpha^{\prime 0*}(t) B_\alpha^{\prime 1}(t) - B_\alpha^{\prime 1*}(t) B_\alpha^{\prime 0}(t) \right) \frac{1}{e^{\beta\omega_\alpha} - 1},
\end{aligned}$$

$$\begin{aligned} \langle J_x(t) \rangle &= \sum_{i,j=0,1} (A_j^{1*}(t)A_i^1(t) - A_j^{0*}(t)A_i^0(t)) \langle a_j^{0\dagger} a_i^0 \rangle_S \\ &\quad + \sum_{i,\alpha} |g_\alpha|^2 (B_\alpha^{1*}(t)B_\alpha^1(t) - B_\alpha^{0*}(t)B_\alpha^0(t)) \frac{1}{e^{\beta\omega_\alpha} - 1}, \end{aligned}$$

$$\text{with } \langle b_\beta^{0\dagger} b_\alpha^0 \rangle_B = \delta_{\alpha\beta} \frac{1}{e^{\beta\omega_\alpha} - 1}.$$

### Appendix C: Individual decoherence: derivations

The evolution of  $c_i(t)$  in the Heisenberg picture fulfills

$$\begin{aligned} \dot{c}_0 &= i [H_{\text{tot}}, c_0] \\ &= -i (\omega_{0,0} + \mu(t) - G_z) c_0 - i G_x c_1 - i \sum_{\alpha} g_{0,\alpha} (b_{0,\alpha}^\dagger + b_{0,\alpha}), \end{aligned} \quad (\text{C1})$$

$$\begin{aligned} \dot{c}_1 &= i [H_{\text{tot}}, c_1] \\ &= -i (\omega_{0,1} + \mu(t) + G_z) c_1 - i G_x c_0 - i \sum_{\alpha} g_{1,\alpha} (b_{1,\alpha}^\dagger + b_{1,\alpha}), \end{aligned} \quad (\text{C2})$$

where

$$\begin{aligned} [J_x, c_0] &= -c_1, [J_z, c_0] = c_0, \\ [J_x, c_1] &= -c_0, [J_z, c_1] = -c_1. \end{aligned}$$

have been used. And the reservoir annihilation operator  $b_{i,\alpha}(t)$  satisfies

$$\begin{aligned} \dot{b}_{i,\alpha} &= i [H_{\text{tot}}, b_{i,\alpha}] \\ &= -i \omega_{i,\alpha} b_{i,\alpha} - i g_{i,\alpha} (c_i^\dagger + c_i). \end{aligned} \quad (\text{C3})$$

By formally integrating Eq. (C3), the equation of motion for the reservoir operator is

$$\begin{aligned} b_{i,\alpha}(t) &= b_{i,\alpha}(0) \exp(-i \omega_{i,\alpha} t) \\ &\quad - i g_{i,\alpha} \int_0^t ds (c_i^\dagger(s) + c_i(s)) \exp(-i \omega_{i,\alpha} (t-s)). \\ b_{i,\alpha}^\dagger(t) &= b_{i,\alpha}^\dagger(0) \exp(i \omega_{i,\alpha} t) \\ &\quad + i g_{i,\alpha} \int_0^t ds (c_i^\dagger(s) + c_i(s)) \exp(i \omega_{i,\alpha} (t-s)). \end{aligned}$$

Substituting the formal solution into Eqs. (C1) and (C2), we have

$$\begin{aligned} \dot{c}_0(t) &= -i (\omega_{0,0} + \mu(t) - G_z) c_0(t) - i G_x c_1(t) \\ &\quad - i \sum_{\alpha} g_{0,\alpha} (b_{0,\alpha}^\dagger(0) \exp(i \omega_{0,\alpha} t) + b_{0,\alpha}(0) \exp(-i \omega_{0,\alpha} t)) \\ &\quad - 2i \int_0^t ds (c_0^\dagger(s) + c_0(s)) \sum_{\alpha} g_{0,\alpha}^2 \sin(\omega_{0,\alpha} (t-s)) \end{aligned}$$

and

$$\begin{aligned} \dot{c}_1(t) &= -i (\omega_{0,1} + \mu(t) + G_z) c_1(t) - i G_x c_0(t) \\ &\quad - i \sum_{\alpha} g_{1,\alpha} (b_{1,\alpha}(0) \exp(-i \omega_{1,\alpha} t) + b_{1,\alpha}^\dagger(0) \exp(i \omega_{1,\alpha} t)) \\ &\quad - 2i \int_0^t ds (c_1^\dagger(s) + c_1(s)) \sum_{\alpha} g_{1,\alpha}^2 \sin(\omega_{1,\alpha} (t-s)) \end{aligned}$$

Inserting the linear expansion of the system operators used in the main text into the equations below yields the coefficient equations for  $C_i^j(t)$ ,  $\bar{C}_i^j(t)$ ,  $B_{i,\alpha}^j(t)$ , and  $\bar{B}_{i,\alpha}^j(t)$ .

### 1. Dynamics in the encoding subspace (individual reservoirs)

We will focus on components in the encoding subspace. We are interested in the coefficients  $C_i^0$  and  $C_i^1$ , whose evolution satisfies

$$\dot{C}_0^0(t) = -i(\omega_{0,0} + \mu(t) - G_z)C_0^0(t) - iG_x C_1^0(t) - \int_0^t ds f_0(t-s)(\bar{C}_0^{0*}(s) + C_0^0(s)), \quad (C4)$$

$$\dot{C}_1^0(t) = -i(\omega_{0,0} + \mu(t) - G_z)C_1^0(t) - iG_x C_1^1(t) - \int_0^t ds f_0(t-s)(\bar{C}_1^{0*}(s) + C_1^0(s)), \quad (C5)$$

$$\dot{C}_0^1(t) = -i(\omega_{0,1} + \mu(t) + G_z)C_0^1(t) - iG_x C_0^0(t) - \int_0^t ds f_1(t-s)(\bar{C}_0^{1*}(s) + C_0^1(s)), \quad (C6)$$

$$\dot{C}_1^1(t) = -i(\omega_{0,1} + \mu(t) + G_z)C_1^1(t) - iG_x C_1^0(t) - \int_0^t ds f_1(t-s)(\bar{C}_1^{1*}(s) + C_1^1(s)). \quad (C7)$$

To apply gate operations on the identical particle qubits (IPQs), we set  $\omega_{0,0} = \omega_{0,1} = 0$ . In the following sections, we will consider three different gate operations: information storage, the X-gate operation, and the Z-gate operation.

#### a. Information storage process.

In this case, the gate operations are not applied, i.e.,  $G_x = G_z = 0$ . The information is encoded in the operator subspace with the basis  $\{c_i^j\}$  at the initial moment, which implies  $C_0^0(0) = C_1^1(0) = 1$ . At this time, the evolutions of  $C_i^j(t)$  are decoupled from each other:

$$\dot{C}_0^0(t) = -i\mu(t)C_0^0(t) - \int_0^t ds f_0(t-s)C_0^0(s) + c_0^0(t),$$

$$\dot{C}_1^0(t) = -i\mu(t)C_1^0(t) - \int_0^t ds f_0(t-s)C_1^0(s) + c_1^0(t),$$

$$\dot{C}_0^1(t) = -i\mu(t)C_0^1(t) - \int_0^t ds f_1(t-s)C_0^1(s) + c_0^1(t),$$

$$\dot{C}_1^1(t) = -i\mu(t)C_1^1(t) - \int_0^t ds f_1(t-s)C_1^1(s) + c_1^1(t),$$

where  $c_i^j(t) = \int_0^t ds f_i(t-s)\bar{C}_i^{j*}(s)$ . Introducing slow variables  $\tilde{C}_i^j(t) = C_i^j(t) \exp\left(-i \int_0^t d\tau \mu(\tau)\right)$ , we obtain

$$\begin{aligned} \dot{\tilde{C}}_i^j(t) &= -\exp\left(-i \int_0^t d\tau \mu(\tau)\right) \\ &\times \int_0^t ds f_i(t-s) \exp\left(i \int_0^s d\tau \mu(\tau)\right) \tilde{C}_i^j(s) + \tilde{c}_i^j(t), \end{aligned}$$

where  $\tilde{c}_i^j(t) = -i \int_0^t ds f_i(t-s)\bar{C}_i^{j*}(s) \exp\left(-i \int_0^t d\tau \mu(\tau)\right)$ .

To address the rapidly oscillating behavior in  $\tilde{c}_i^j(t)$ , we focus on the dynamical equation for  $\bar{C}_i^{j*}$ , given by

$$\dot{\bar{C}}_i^{j*}(t) = i\mu(t)\bar{C}_i^{j*}(t) - \int_0^t ds f_i^*(t-s)(C_i^j(s) + \bar{C}_i^{j*}(s)).$$

It appears that  $\bar{C}_i^{j*}(s)$  contains oscillating terms such as  $\exp\left(i \int_0^s d\tau \mu(\tau)\right)$ , leading to  $\tilde{c}_i^j(t) \rightarrow 0$ . As a result, the information encoded in the operator subspace is robust against individual noise at finite reservoir temperature. We can express this as a vector equation

$$\begin{aligned} \dot{\tilde{\bar{C}}}(t) &= -\exp\left(-i \int_0^t d\tau \mu(\tau)\right) \\ &\times \int_0^t ds \bar{f}(t-s) \exp\left(i \int_0^s d\tau \mu(\tau)\right) \tilde{\bar{C}}(s) + \tilde{\bar{c}}(t), \end{aligned} \quad (C8)$$

with  $\vec{C}(t) = [\tilde{C}_1^1(t), \tilde{C}_0^1(t), \tilde{C}_1^0(t), \tilde{C}_0^0(t)]$ ,  $\vec{c}(t) = [\tilde{c}_1^1(t), \tilde{c}_1^0(t), \tilde{c}_0^1(t), \tilde{c}_0^0(t)]$ , and

$$\bar{f} = \text{diag}(f_1, f_1, f_0, f_0).$$

b. *The Z-Gate Operation.*

When we consider Z-gate operation on the IPQ, it requires  $G_x = 0$ , leading to the following equations

$$\begin{aligned}\dot{C}_0^0(t) &= -i(\mu(t) - G_z)C_0^0(t) - \int_0^t ds f_0(t-s)(\bar{C}_0^{0*}(s) + C_0^0(s)), \\ \dot{C}_1^0(t) &= -i(\mu(t) - G_z)C_1^0(t) - \int_0^t ds f_0(t-s)(\bar{C}_1^{0*}(s) + C_1^0(s)), \\ \dot{C}_0^1(t) &= -i(\mu(t) + G_z)C_0^1(t) - \int_0^t ds f_1(t-s)(\bar{C}_0^{1*}(s) + C_0^1(s)), \\ \dot{C}_1^1(t) &= -i(\mu(t) + G_z)C_1^1(t) - \int_0^t ds f_1(t-s)(\bar{C}_1^{1*}(s) + C_1^1(s)).\end{aligned}$$

Similar to information storage, the information is encoded in the operator subspace with the basis  $\{c_i^0\}$ . We introduce  $\tilde{C}_i^j(t)$  with the same definition as before. Therefore, we have

$$\begin{aligned}\dot{\tilde{C}}_i^0(t) &= iG_z\tilde{C}_i^0(t) - \exp\left(-i\int_0^t d\tau\mu(\tau)\right)\int_0^t ds f_0(t-s)\exp\left(i\int_0^s d\tau\mu(\tau)\right)\tilde{C}_i^0(s) + \tilde{c}_i^0(t), \\ \dot{\tilde{C}}_i^1(t) &= -iG_z\tilde{C}_i^1(t) - \exp\left(-i\int_0^t d\tau\mu(\tau)\right)\int_0^t ds f_1(t-s)\exp\left(i\int_0^s d\tau\mu(\tau)\right)\tilde{C}_i^1(s) + \tilde{c}_i^1(t).\end{aligned}$$

These can be written in vector form as

$$\dot{\vec{\tilde{C}}}(t) = -iG_z\bar{\sigma}_z \otimes \bar{I}_2\vec{\tilde{C}}(t) - \exp\left(-i\int_0^t d\tau\mu(\tau)\right)\int_0^t ds \exp\left(i\int_0^s d\tau\mu(\tau)\right)\bar{f}(t-s)\vec{\tilde{C}}(s) + \vec{\tilde{c}}(t),$$

with the same variables used in Eq. (C8). Due to the rapidly oscillating terms in the convolution, the second and third terms in the above equations contribute negligibly to the Z-gate operation. Therefore, the effective dynamics can be described by

$$\dot{\vec{\tilde{C}}}(t) = -iG_z\bar{\sigma}_z \otimes \bar{I}_2\vec{\tilde{C}}(t),$$

which represents a perfect Z-gate operation on the IPQs without decoherence effects.

c. *The X-Gate operation.*

We consider the X-gate operation with  $G_z = 0$ . Since the information needs to be transferred between  $c_0^0$  and  $c_1^0$ , we must account for all the expansion coefficients of  $c_0^0$  and  $c_1^0$ , whose dynamics are described by Eqs. (C4 - C7), i.e.,

$$\begin{aligned}\dot{C}_0^0(t) &= -i\mu(t)C_0^0(t) - iG_xC_0^1(t) - \int_0^t ds f_0(t-s)(\bar{C}_0^{0*}(s) + C_0^0(s)), \\ \dot{C}_1^0(t) &= -i\mu(t)C_1^0(t) - iG_xC_1^1(t) - \int_0^t ds f_0(t-s)(\bar{C}_1^{0*}(s) + C_1^0(s)), \\ \dot{C}_0^1(t) &= -i\mu(t)C_0^1(t) - iG_xC_0^0(t) - \int_0^t ds f_1(t-s)(\bar{C}_0^{1*}(s) + C_0^1(s)), \\ \dot{C}_1^1(t) &= -i\mu(t)C_1^1(t) - iG_xC_1^0(t) - \int_0^t ds f_1(t-s)(\bar{C}_1^{1*}(s) + C_1^1(s)).\end{aligned}$$

We can rewrite these equations in vector form

$$i\dot{\vec{C}}(t) = (\mu(t)\bar{I}_4 + G_x\bar{\sigma}_x \otimes \bar{I}_2)\vec{C}(t) + 2\int_0^t ds \bar{f}(t-s)\vec{C}(s) + \vec{c}(t).$$

Using the unitary matrix

$$\bar{U}_X = \frac{\sqrt{2}}{2} \begin{pmatrix} 1 & 0 & -1 & 0 \\ 0 & 1 & 0 & -1 \\ 1 & 0 & 1 & 0 \\ 0 & 1 & 0 & 1 \end{pmatrix},$$

the vector equation can be transformed into

$$\dot{\vec{D}}(t) = -i (\mu(t)\bar{I}_4 + G_x \bar{\sigma}_z \otimes \bar{I}_2) \vec{D}(t) - \int_0^t ds \bar{F}(t-s) \vec{D}(s) + \vec{d}(t),$$

with  $\vec{D}(t) = \bar{U}_X \vec{C}$ ,  $\vec{d} = \bar{U}_X \vec{c}$ , and

$$\bar{F} = \frac{1}{2} \begin{pmatrix} f_0 + f_1 & 0 & f_1 - f_0 & 0 \\ 0 & f_0 + f_1 & 0 & f_1 - f_0 \\ f_1 - f_0 & 0 & f_0 + f_1 & 0 \\ 0 & f_1 - f_0 & 0 & f_0 + f_1 \end{pmatrix}.$$

By defining  $\tilde{\vec{D}}(t) = \vec{D}(t) \exp(-i \int_0^t d\tau \mu(\tau))$ , we arrive at

$$\begin{aligned} \dot{\tilde{\vec{D}}}(t) &= -i G_x \bar{\sigma}_z \otimes \bar{I}_2 \tilde{\vec{D}}(t) \\ &\quad - \exp\left(-i \int_0^t d\tau \mu(\tau)\right) \int_0^t ds \exp\left(i \int_0^s d\tau \mu(\tau)\right) \bar{F}(t-s) \tilde{\vec{D}}(s) + \tilde{\vec{d}}(t), \end{aligned}$$

where

$$\tilde{\vec{d}}(t) = -\exp\left(-i \int_0^t d\tau \mu(\tau)\right) \int_0^t ds \exp\left(-i \int_0^s d\tau \mu(\tau)\right) \bar{F}(t-s) \vec{d}(s).$$

With the slow variables defined as

$$\tilde{\vec{C}}_i^{j*}(s) = \bar{C}_i^{j*}(s) \exp\left(i \int_0^s d\tau \mu(\tau)\right), \quad (\text{C9})$$

the rapid oscillations caused by  $\exp(\pm i \int_0^s d\tau \mu(\tau))$  result in the cancellation of the last two terms in  $\dot{\tilde{\vec{D}}}(t)$  during the evolution. Then, we obtain a more concise effective form.

$$\dot{\tilde{\vec{D}}}(t) = -i G_x \bar{\sigma}_z \otimes \bar{I}_2 \tilde{\vec{D}}(t).$$

When we transform the variable  $\vec{D}$  back into  $\vec{C} = \bar{U}_D^\dagger \vec{D}$ , we arrive at a perfect  $X$ -gate operation:

$$\vec{C}(t) = -i G_x \bar{\sigma}_x \otimes \bar{I}_2 \vec{C}(t).$$

## 2. Gate-operation dynamics

In this subsection, we consider a simplified case where the counter-rotating wave terms in the interaction Hamiltonian are neglected. At this time, the annihilation operators can be expanded solely in terms of the initial annihilation operators, i.e.,

$$\begin{aligned} c_j(t) &= \sum_{i=0,1} C_i^j(t) c_i^0 + \sum_{i,\alpha} B_{i,\alpha}^j(t) b_{i,\alpha}^0, \\ c_j^\dagger(t) &= \sum_{i=0,1} C_i^{j*}(t) c_i^{0\dagger} + \sum_{i,\alpha} B_{i,\alpha}^{j*}(t) b_{i,\alpha}^{0\dagger}. \end{aligned}$$

The dynamical equations of the coefficients reads

$$\begin{aligned}\dot{C}_i^0(t) &= -i(\mu(t) - G_z)C_i^0(t) - iG_x C_i^1(t) - \int ds f_0(t-s)C_i^0(s), \\ \dot{B}_{0,\alpha}^0(t) &= -i(\mu(t) - G_z)B_{0,\alpha}^0(t) - iG_x B_{0,\alpha}^1(t) - \int_0^t ds f_0(t-s)B_{0,\alpha}^0(s) \\ &\quad - i g_{0,\alpha} \exp(-i\omega_{0,\alpha}t),\end{aligned}\tag{C10}$$

$$\begin{aligned}\dot{B}_{1,\alpha}^0(t) &= -i(\mu(t) - G_z)B_{1,\alpha}^0(t) - iG_x B_{1,\alpha}^1(t) - \int_0^t ds f_0(t-s)B_{1,\alpha}^0(s) \\ \dot{C}_i^1(t) &= -i(\mu(t) + G_z)C_i^1(t) - iG_x C_i^0(t) - \int_0^t ds f_1(t-s)C_i^1(s), \\ \dot{B}_{0,\alpha}^1(t) &= -i(\mu(t) + G_z)B_{0,\alpha}^1(t) - iG_x B_{0,\alpha}^0(t) - \int_0^t ds f_1(t-s)B_{0,\alpha}^1(s), \\ \dot{B}_{1,\alpha}^1(t) &= -i(\mu(t) + G_z)B_{1,\alpha}^1(t) - iG_x B_{1,\alpha}^0(t) - \int_0^t ds f_1(t-s)B_{1,\alpha}^1(s), \\ &\quad - i g_{1,\alpha} \exp(-i\omega_{1,\alpha}t).\end{aligned}\tag{C11}$$

In what follows, we simulate the average value of the observable variants  $\langle J_x(t) \rangle$ ,  $\langle J_y(t) \rangle$ , and  $\langle J_z(t) \rangle$ , where  $\langle J_k(t) \rangle = \text{Tr}\{J_k(t)\rho_{\text{tot}}\}$ . We set that the system and heat reservoirs are not correlated each other and the total density matrix is written as  $\rho_{\text{tot}} = \rho_S(0) \otimes \rho_B^0(0) \otimes \rho_B^1(0)$ , and the reservoir is prepared on the thermal equilibrium state

$$\rho_B^k(0) = \sum_{n,\alpha} \frac{e^{-\beta_k \omega_{k,\alpha}}}{1 - e^{-\beta_k \omega_{k,\alpha}}} |n_{k,\alpha}\rangle \langle n_{k,\alpha}|,$$

where  $\beta_k$  is the inverse reservoir temperature and  $|n_k\rangle$  is the fock state with particle number  $n_k$ .

#### a. The Z-gate operation.

We analyze the expected values of the Pauli operators within the context of the Z-gate operation. The z-component is defined as

$$\langle J_z(t) \rangle = \langle c_1^\dagger(t)c_1(t) - c_0^\dagger(t)c_0(t) \rangle,$$

which can be expressed as

$$\begin{aligned}&= \sum_{i,j=0}^1 (C_j^{1*}(t)C_i^1(t) - C_j^{0*}(t)C_i^0(t)) \langle c_j^\dagger c_i \rangle_S \\ &\quad + \sum_{i,\alpha} (|B_{i,\alpha}^1(t)|^2 - |B_{i,\alpha}^0(t)|^2) \langle b_{i,\alpha}^\dagger b_{i,\alpha} \rangle_B,\end{aligned}$$

where we have considered that  $\text{Tr}_B\{b_{j,\beta}^{0\dagger} b_{i,\alpha}^0 \rho_B(0)\} = \delta_{\alpha\beta} \delta_{ij}$ .  $B_{j,\beta}^i$  can be calculated using the Laplace transformation. By applying the Laplace transformation to Eqs. (C10) and (C11), we obtain

$$\begin{aligned}\tilde{B}_{1,\alpha}^1(t_1) &= \frac{-ig_{1,\alpha}}{(t_1 + i\omega_{1,\alpha}) \left( t_1 + \tilde{f}_1(t_1) + i(\mu + G_z) \right)}, \\ \tilde{B}_{0,\alpha}^0(t_1) &= \frac{-ig_{0,\alpha}}{(t_1 + i\omega_{0,\alpha}) \left( t_1 + \tilde{f}_0(t_1) + i(\mu - G_z) \right)},\end{aligned}$$

where  $\tilde{f}_j(t_1)$  represents the Laplace transformation of the correlation function for the  $j$ -th reservoir, and we have assumed  $B_{i,\alpha}^j(0) = 0$ . Since  $B_{i,\alpha}^j(0) = 0$ , it follows that  $B_1^0(t) = B_0^1(t) = 0$ . If the correlation function  $f_j(t-s)$

is specified, the solution can be derived by taking the inverse Laplace transformation of  $\tilde{B}_{i,\alpha}^j(t_1)$ , i.e.,  $B_{j,\beta}^i(t) = \mathcal{L}^{-1}[\tilde{B}_{i,\alpha}^j(t_1)]$ . By introducing

$$\begin{aligned}\tilde{B}'_{1,\alpha}{}^1(t_1) &= \frac{1}{(t_1 + i\omega_{1,\alpha}) \left( t_1 + \tilde{f}_1(t_1) + i(\mu + G_z) \right)}, \\ \tilde{B}'_{0,\alpha}{}^0(t_1) &= \frac{1}{(t_1 + i\omega_{0,\alpha}) \left( t_1 + \tilde{f}_0(t_1) + i(\mu - G_z) \right)},\end{aligned}$$

we see that  $B_{j,\beta}^i(t) = -ig_{i,\alpha}B'_{j,\beta}{}^i(t)$  with  $B'_{j,\beta}{}^i(t) = \mathcal{L}^{-1}[\tilde{B}'_{j,\alpha}{}^i(t_1)]$ , leading to the expressions reported in the main text, Eqs. (24) and (25).

where  $B_1^0(t) = B_1^0(t) = 0$  and  $\langle b_{j,\beta}^{0\dagger} b_{i,\alpha}^0 \rangle_B = \delta_{\alpha\beta} \delta_{ij} \frac{1}{e^{\beta_0 \omega_{j,\alpha}} - 1}$  have been utilized.

*b. The X-gate operation.*

In this case, the dynamics of  $B_{j,\alpha}^i(t)$  is different to the Z-gate operation case. We divid the dynamical equations into two independent groups. One is

$$\begin{aligned}\dot{B}_{0,\alpha}^0(t) &= -i\mu B_{0,\alpha}^0(t) - iG_x B_{0,\alpha}^1(t) - \int_0^t ds f_0(t-s) B_{0,\alpha}^0(s) \\ &\quad - i g_{0,\alpha} \exp(-i\omega_{0,\alpha}t), \\ \dot{B}_{0,\alpha}^1(t) &= -i\mu B_{0,\alpha}^1(t) - iG_x B_{0,\alpha}^0(t) - \int_0^t ds f_1(t-s) B_{0,\alpha}^1(s),\end{aligned}$$

and another one reads

$$\begin{aligned}\dot{B}_{1,\alpha}^1(t) &= -i\mu B_{1,\alpha}^1(t) - iG_x B_{1,\alpha}^0(t) - \int_0^t ds f_1(t-s) B_{1,\alpha}^1(s), \\ &\quad - i g_{1,\alpha} \exp(-i\omega_{1,\alpha}t). \\ \dot{B}_{1,\alpha}^0(t) &= -i\mu B_{1,\alpha}^0(t) - iG_x B_{1,\alpha}^1(t) - \int_0^t ds f_0(t-s) B_{1,\alpha}^0(s),\end{aligned}$$

which can be solved by the Laplace transformation.

$$\begin{aligned}\tilde{B}_{0,\alpha}^0(t_1) &= \frac{i g_{0,\alpha} \left( t_1 + i\mu + \tilde{f}_1(t_1) \right)}{(t_1 + i\omega_{0,\alpha}) \left( G_x^2 + \left( t_1 + i\mu + \tilde{f}_0(t_1) \right) \left( t_1 + i\mu + \tilde{f}_1(t_1) \right) \right)}, \\ \tilde{B}_{0,\alpha}^1(t_1) &= \frac{i G_x g_{0,\alpha}}{(t_1 + i\omega_{0,\alpha}) \left( G_x^2 + \left( t_1 + i\mu + \tilde{f}_0(t_1) \right) \left( t_1 + i\mu + \tilde{f}_1(t_1) \right) \right)}, \\ \tilde{B}_{1,\alpha}^0(t_1) &= \frac{i G_x g_{1,\alpha}}{(t_1 + i\omega_{1,\alpha}) \left( G_x^2 + \left( t_1 + i\mu + \tilde{f}_0(t_1) \right) \left( t_1 + i\mu + \tilde{f}_1(t_1) \right) \right)}, \\ \tilde{B}_{1,\alpha}^1(t_1) &= \frac{i g_{1,\alpha} \left( t_1 + i\mu + \tilde{f}_0(t_1) \right)}{(t_1 + i\omega_{1,\alpha}) \left( G_x^2 + \left( t_1 + i\mu + \tilde{f}_0(t_1) \right) \left( t_1 + i\mu + \tilde{f}_1(t_1) \right) \right)}.\end{aligned}$$

where  $\tilde{f}_k(t_1) = \mathcal{L}[f_k(t)]$  is the Laplace transform of  $f_k(t)$ , and the initial conditions  $B_j^i(0) = 0$  have been used. If  $f_k(t)$  is known, the solutions can be obtained via the inverse Laplace transformation. The mean values of  $\{J_z\}$  are given

by

$$\begin{aligned}
\langle J_x(t) \rangle &= \sum_{i,j=0,1} (C_i^{1*}(t)C_j^0(t) + C_i^{0*}(t)C_j^1(t)) \langle c_i^{0\dagger}c_j^0 \rangle_S \\
&\quad + \sum_{i,\alpha} |g_{i,\alpha}|^2 \left( B_{i,\alpha}^{\prime 0*}(t)B_{i,\alpha}^{\prime 1}(t) + B_{i,\alpha}^{\prime 1*}(t)B_{i,\alpha}^{\prime 0}(t) \right) \frac{1}{e^{\beta_i \omega_{i,\alpha}} - 1}, \\
\langle J_y(t) \rangle &= \sum_{i,j=0,1} i (C_i^{1*}(t)C_j^0(t) - C_i^{0*}(t)C_j^1(t)) \langle c_i^{0\dagger}c_j^0 \rangle_S \\
&\quad + \sum_{i,\alpha} i |g_{i,\alpha}|^2 (B_{i,\alpha}^{\prime 0*}(t)B_{i,\alpha}^{\prime 1}(t) - B_{i,\alpha}^{\prime 1*}(t)B_{i,\alpha}^{\prime 0}(t)) \frac{1}{e^{\beta_i \omega_{i,\alpha}} - 1}, \\
\langle J_z(t) \rangle &= \sum_{i,j=0,1} (C_j^{1*}(t)C_i^1(t) - C_j^{0*}(t)C_i^0(t)) \langle c_j^{0\dagger}c_i^0 \rangle_S \\
&\quad + \sum_{i,\alpha} |g_{i,\alpha}|^2 (B_{i,\alpha}^{\prime 1*}(t)B_{i,\alpha}^{\prime 1}(t) - B_{i,\alpha}^{\prime 0*}(t)B_{i,\alpha}^{\prime 0}(t)) \frac{1}{e^{\beta_i \omega_{i,\alpha}} - 1},
\end{aligned}$$

$$\text{with } \langle b_{j,\beta}^{0\dagger}b_{i,\alpha}^0 \rangle_B = \delta_{\alpha\beta} \delta_{ij} \frac{1}{e^{\beta_j \omega_{j,\alpha}} - 1}.$$

#### Appendix D: Initial states and expectation values

We assume that the initial system state is a pure state which can be written as  $\rho_S(0) = |\psi(0)\rangle\langle\psi(0)|$  with  $|\psi(0)\rangle = \alpha_0 c_0^{0\dagger}|00\rangle + \alpha_1 c_1^{0\dagger}|00\rangle$ . Here,  $\alpha_0$  and  $\alpha_1$  are arbitrary complex amplitudes fulfilling  $|\alpha_1|^2 + |\alpha_0|^2 = 1$ . Thus we have

$$\begin{aligned}
\langle a_i^{0\dagger}a_j^0 \rangle_S &= \text{Tr}_S \left\{ a_i^{0\dagger}a_j^0 \rho_S(0) \right\} \\
&= \langle \psi(0) | a_i^{0\dagger}a_j^0 | \psi(0) \rangle \\
&= \frac{1}{2} \sum_{k,l} \alpha_k^* \alpha_l \langle 00 | \left( c_k^0 c_1^{0\dagger} c_1^0 c_l^{0\dagger} - (-1)^i c_k^0 c_0^{0\dagger} c_1^0 c_l^{0\dagger} - (-1)^j c_k^0 c_1^{0\dagger} c_0^0 c_l^{0\dagger} + (-1)^{i+j} c_k^0 c_0^{0\dagger} c_0^0 c_l^{0\dagger} \right) c_l^{0\dagger} | 00 \rangle \\
&= \frac{1}{2} \sum_{k,l} \alpha_k^* \alpha_l (\delta_{k1} \delta_{l1} - (-1)^i \delta_{k0} \delta_{l1} - (-1)^j \delta_{k1} \delta_{l0} + (-1)^{i+j} \delta_{k0} \delta_{l0}) \\
&= \frac{1}{2} (\alpha_1^* \alpha_1 - (-1)^i \alpha_0^* \alpha_1 - (-1)^j \alpha_1^* \alpha_0 + (-1)^{i+j} \alpha_0^* \alpha_0),
\end{aligned}$$

which can be used to determine the mean values of the system part. The mixed initial system state can be written as  $\rho_S(0) = \sum_{kl} \rho_{kl} c_k^{0\dagger} |00\rangle \langle 00| c_l^0$ , which leads to

$$\begin{aligned}
\langle a_i^{0\dagger}a_j^0 \rangle_S &= \text{Tr}_S \left\{ a_i^{0\dagger}a_j^0 \rho_S(0) \right\} \\
&= \frac{1}{2} \sum_{kl} \rho_{kl} \langle 00 | c_l^0 \left( c_1^\dagger - (-1)^i c_0^\dagger \right) (c_1 - (-1)^j c_0) c_k^{0\dagger} | 00 \rangle \\
&= \frac{1}{2} \sum_{kl} \rho_{kl} \langle 00 | c_l^0 \left( c_1^\dagger c_1 - (-1)^j c_1^\dagger c_0 - (-1)^i c_0^\dagger c_1 + (-1)^{j+i} c_0^\dagger c_0 \right) c_k^{0\dagger} | 00 \rangle \\
&= \frac{1}{2} (\rho_{11} - (-1)^j \rho_{01} - (-1)^i \rho_{10} + (-1)^{j+i} \rho_{00})
\end{aligned}$$

---

[1] M. Schlosshauer, Quantum decoherence, Phys. Rep. **831**, 1 (2019).

[2] S. Cao, B. Wu, F. Chen, M. Gong, Y. Wu, Y. Ye, C.

- Zha, H. Qian, C. Ying, and S. Guo *et al.*, Generation of genuine entanglement up to 51 superconducting qubits, *Nature* **619**, 738 (2023).
- [3] J. J. Garcia-Ripoll and J. I. Cirac, Quantum computation with cold bosonic atoms in an optical lattice, *Philos. Trans. R. Soc. A* **361**, 1537 (2003).
- [4] N. Arunkumar, K. S. Olsson, J. T. Oon, C. A. Hart, D. B. Bucher, D. R. Glenn, M. D. Lukin, H. Park, D. Ham, and R. L. Walsworth, Quantum logic enhanced sensing in solid-state spin ensembles, *Phys. Rev. Lett.* **131**, 100801 (2023).
- [5] S. Jain, T. Säggerer, P. Hrmo, C. Torkzaban, M. Stadler, R. Oswald, C. Axline, A. Bautista-Salvador, C. Ospelkaus, D. Kienzler, and J. Home, Penning micro-trap for quantum computing, *Nature (London)* **627**, 510 (2024).
- [6] N. P. de Leon, K. M. Itoh, D. Kim, K. K. Mehta, T. E. Northup, H. Paik, B. S. Palmer, N. Samarth, S. Sangtawesin, and D. W. Steerman, Materials challenges and opportunities for quantum computing hardware, *Science* **372**, eabb2823 (2021).
- [7] M. H. Michael *et al.*, New Class of Quantum Error-Correcting Codes for a Bosonic Mode, *Phys. Rev. X* **6**, 031006 (2016).
- [8] Yong Li, Lian-Ao Wu, Ying-Dan Wang and Li-Ping Yang, Nondeterministic ultrafast ground-state cooling of a mechanical resonator, *Physical Review B* **84**, 094502 (2011).
- [9] Jin-Shi Xu *et al.* Demon-like Algorithmic Quantum Cooling and its Realization with Quantum Optics, *Nature Photonics* **8**, 113-118 (2014)
- [10] A. Paetznick *et al.*, Demonstration of logical qubits and repeated error correction with better-than-physical error rates, arXiv:2404.02280 (2024).
- [11] J. Preskill *et al.*, Hardware-efficient quantum error correction via concatenated bosonic qubits, *Nature*, online 2025.
- [12] Z. Ni *et al.*, Beating the break-even point with a discrete-variable-encoded logical qubit, *Nature* **616**, 56 (2023).
- [13] B. L. Brock *et al.*, Quantum error correction of qudits beyond break-even, *Nature* **641**, 612 (2025).
- [14] E. Knill, R. Laflamme, and G. J. Milburn, A scheme for efficient quantum computation with linear optics, *Nature (London)* **409**, 46 (2001).
- [15] J. H. Shapiro, Single-photon Kerr nonlinearities do not help quantum computation, *Phys. Rev. A* **73**, 062305 (2006).
- [16] J. D. Teoh *et al.*, Dual-rail encoding with superconducting cavities, *PNAS* **120** (41), e2221736120 (2023).
- [17] K. S. Chou, T. Shemma, H. McCarrick, *et al.*, A superconducting dual-rail cavity qubit with erasure-detected logical measurements, *Nat. Phys.* **20**, 1454 (2024).
- [18] M. Grassl, T. Beth, and T. Pellizzari, Codes for the quantum erasure channel, *Phys. Rev. A* **56**, 33 (1997).
- [19] Y. Li, P. C. Humphreys, G. J. Mendoza, and S. C. Benjamin, Resource costs for fault-tolerant linear optical quantum computing, *Phys. Rev. X* **5**, 041007 (2015).
- [20] S. Bartolucci *et al.*, Fusion-based quantum computation, *Nat. Commun.* **14**, 912 (2023).
- [21] C. Berdou *et al.*, One hundred second bit-flip time in a two-photon dissipative oscillator, *PRX Quantum* **4**, 020350 (2023).
- [22] P. Reinhold *et al.*, Error-corrected gates on an encoded qubit, *Nat. Phys.* **16**, 822 (2020).
- [23] M. Bartkowiak, L.-A. Wu, A. Miranowicz, Quantum circuits for amplification of Kerr nonlinearity via quadrature squeezing, *J. Phys. B* **47**, 012332 (2009).
- [24] L.-A. Wu, A. Miranowicz, X. B. Wang, Y.-x. Liu, F. Nori, Perfect function transfer and interference effects in interacting boson lattices, *Phys. Rev. A* **80**, 145501 (2014).
- [25] Y. Lin, D. R. Leibbrandt, D. Leibfried, and C. W. Chou, Quantum entanglement between an atom and a molecule, *Nature (London)* **581**, 273 (2020).
- [26] L. Sun *et al.*, Tracking photon jumps with repeated quantum non-demolition parity measurements, *Nature* **511**, 444 (2014).
- [27] T. Proctor, K. Rudinger, K. Young, M. Sarovar, and R. Blume-Kohout, What randomized benchmarking actually measures, *Phys. Rev. Lett.* **119**, 130502 (2017).
- [28] M. Friesen, J. Ghosh, M. A. Eriksson, and S. N. Coppersmith, A decoherence-free subspace in a charge quadrupole qubit, *Nat. Commun.* **8**, 15923 (2017).
- [29] N. Ezzell, B. Pokharel, L. Tewala, G. Quiroz, and D. A. Lidar, Dynamical decoupling for superconducting qubits: A performance survey, *Phys. Rev. Applied* **20**, 064027 (2023).
- [30] L. -A. Wu, M. S. Byrd, and D. A. Lidar, Efficient universal leakage elimination for physical and encoded qubits, *Phys. Rev. Lett.* **89**, 127901 (2002).
- [31] J. Jing, L. -A. Wu, M. Byrd, J. Q. You, T. Yu, and Z. M. Wang, Nonperturbative leakage elimination operators and control of a three-level system, *Phys. Rev. Lett.* **114**, 190502 (2015).
- [32] L. -A. Wu and D. Lidar, Creating Decoherence-Free Subspaces Using Strong and Fast Pulses, *Phys. Rev. Lett.* **88**, 207902 (2002).
- [33] A. D. C. Tosta, D. J. Brod, and E. F. Galvão, Quantum computation from fermionic anyons on a one-dimensional lattice, *Phys. Rev. A* **99**, 062335 (2019).
- [34] L.-A. Wu and D. Lidar, Qubits as parafermions, *J. Math. Phys.* **43**, 4506 (2002).
- [35] See Supplemental Material at xxx for additional details.
- [36] T. Tsunoda, J. D. Teoh, W. D. Kalfus, S. J. de Graaf, B. J. Chapman, J. C. Curtis, N. Thakur, S. M. Girvin, and R. J. Schoelkopf, Bosonic quantum error correction with cat codes, *PRX Quantum* **4**, 020354 (2023).
- [37] A. Kubica, A. Haim, Y. Vaknin, H. Levine, F. Brandão, and A. Retzker, Erasure Qubits: Overcoming the  $T_1$  Limit in Superconducting Circuits, *Phys. Rev. X* **13**, 041022 (2023).
- [38] J. M. Lukens and P. Lougovski, Frequency-encoded photonic qubits for scalable quantum information processing, *Optica* **4**, 8 (2017).
- [39] J. Ilves, S. Kono, Y. Sunada, S. Yamazaki, M. Kim, K. Koshino, and Y. Nakamura, On-demand generation and characterization of a microwave time-bin qubit, *Npj Quantum Inf.* **6**, 34 (2020).
- [40] F. Scala, D. Nigro, and D. Gerace, Deterministic entangling gates with nonlinear quantum photonic interferometers, *Commun. Phys.* **7**, 118 (2024).
- [41] P. W. Shor, Scheme for reducing decoherence in quantum computer memory, *Phys. Rev. A* **52**, R2493(R) (1995).
- [42] C. Ryan-Anderson *et al.*, Realization of real-time fault-tolerant quantum error correction, *Phys. Rev. X* **11**, 041058 (2021).
- [43] B. de Neeve, T. L. Nguyen, T. Behrle, and J. P. Home, Error correction of a logical grid state qubit by dissipative pumping, *Nat. Phys.* **18**, 296 (2022).
- [44] Google Quantum AI and Collaborators. Quantum error

- correction below the surface code threshold. *Nature* **638**, 920 (2025).
- [45] B. M. Terhal, Quantum error correction for quantum memories, *Rev. Mod. Phys.* **87**, 307 (2015).
- [46] K. Børkje, Scheme for steady-state preparation of a harmonic oscillator in the first excited state, *Phys. Rev. A* **90**, 023806 (2014).
- [47] L. Latmiral and F. Mintert, Deterministic preparation of highly non-classical macroscopic quantum states, *Npj Quantum Inf.* **4**, 44 (2018).
- [48] H. N. Xiong, W. M. Zhang, X. Wang, and M. H. Wu, Exact non-Markovian cavity dynamics strongly coupled to a reservoir, *Phys. Rev. A* **82**, 012105 (2010).
- [49] L. Ferialdi, Dissipation in the Caldeira-Leggett model, *Phys. Rev. A* **95**, 052109 (2017).
- [50] F. Otterpohl, P. Nalbach, and M. Thorwart, Coherent phonon dynamics in optomechanical systems, *Phys. Rev. Lett.* **129**, 120406 (2022).
- [51] Z. M. Wang, S. L. Wu, M. S. Byrd, L. A. Wu, Analytical solutions of bilinear bosonic models and exact characterization of non-Markovian dynamics, *Phys. Rev. A* **111**, 062206 (2025).
- [52] D. Burgarth, P. Facchi, M. Ligabò, and D. Lonigro, Hidden non-Markovianity in open quantum systems, *Phys. Rev. A* **103**, 012203 (2021).
- [53] D. Suter and G. A. Álvarez, Colloquium: Protecting quantum information against environmental noise, *Rev. Mod. Phys.* **88**, 041001 (2016).
- [54] S. S. Zheng, Q. Y. He, M. S. Byrd, and L. A. Wu, Nonperturbative leakage elimination for a logical qubit encoded in a mechanical oscillator, *Phys. Rev. Res.* **2**, 033378 (2020).
- [55] J. Alicea, Y. Oreg, G. Refael, F. von Oppen and M. P. A. Fisher, Non-Abelian statistics and topological quantum information processing in 1D wire networks, *Nat. Phys.* **7**, 412 (2011).
- [56] I. S. Gradshteyn and I. M. Ryzhik, *Table of Integrals, Series, and Products* (Academic Press, New York, 1980).
- [57] J. W. Brown and R. V. Churchill, *Fourier Series and Boundary Value Problems* (McGraw-Hill, New York, 1993).
- [58] Z. M. Wang, M. S. Byrd, J. Jing, and L. -A. Wu, Adiabatic leakage elimination operator in an experimental framework, *Phys. Rev. A* **97**, 062312 (2018).
- [59] Z. M. Wang, M. S. Sarandy, and L. -A. Wu, Almost exact state transfer in a spin chain via pulse control, *Phys. Rev. A* **102**, 022601 (2020).
- [60] M. Heuck, K. Jacobs, and D. R. Englund, Controlled-phase gate using dynamically coupled cavities and optical nonlinearities, *Phys. Rev. Lett.* **124**, 160501 (2020).
- [61] K. Kaur, T. Sépulcre, N. Roch, I. Snyman, S. Florens, and S. Bera, Spin-boson quantum phase transition in multilevel superconducting qubits, *Phys. Rev. Lett.* **127**, 237702 (2021).
- [62] W. L. Ma, S. Puri, R. J. Schoelkopf, M. H. Devoret, S. M. Girvin, and L. Jiang, Quantum control of bosonic modes with superconducting circuits, *Sci. Bull.* **66**, 1789 (2021).
- [63] T. K. Konar, L. G. C. Lakkaraju, S. Ghosh, and A. Sen De, Quantum battery with ultracold atoms: Bosons versus fermions, *Phys. Rev. A* **106**, 022618 (2022).
- [64] I. Bloch, J. Dalibard, and W. Zwerger, Many-body physics with ultracold gases, *Rev. Mod. Phys.* **80**, 885 (2008).
- [65] A. Blais, A. L. Grimsmo, S. M. Girvin, and A. Wallraff, Circuit quantum electrodynamics, *Rev. Mod. Phys.* **93**, 025005 (2021).
- [66] M. Aspelmeyer, T. J. Kippenberg, and F. Marquardt, Cavity optomechanics, *Rev. Mod. Phys.* **86**, 1391 (2014).
- [67] J. Koch, T. M. Yu, J. Gambetta, A. A. Houck, D. I. Schuster, J. Majer, A. Blais, M. H. Devoret, S. M. Girvin, and R. J. Schoelkopf, Charge-insensitive qubit design derived from the Cooper pair box, *Phys. Rev. A* **76**, 042319 (2007).